Supporting Information

Degradation of organic pollutants using a ternary heterojunction catalyst ($CoS_2/CoCo_2O_4$-$MnFe_2O_4$) for activated peroxymonosulfate with magnetic separation, anti-ion interference, and low ion leaching

Ying Shen [a, ‡], Fan Qiu [a, ‡], Yang Fan [a], Yaming Wang [a], Jiawei Kang [a], Mengdie Yang [a], Junjie Chen [a], Haiou Song [b, *], Shupeng Zhang [a, *]

[a] *School of Chemistry and Chemical Engineering, Nanjing University of Science and Technology, Nanjing 210094, China*

[b] *School of Environment, Nanjing Normal University, Nanjing, 210097, PR China*

‡ Y. Shen and F. Qiu contributed equally to this work.

* Corresponding authors.

Tel/Fax: +86 25 84315036

E-mail address: songhaiou2011@126.com (H.O. Song)

shupeng_2006@126.com (S.P Zhang)

1 Experiment

1.1 Materials

Cobalt nitrate hexahydrate ($Co(NO_3)_2·6H_2O$, A.R., Sinopanax Chemical Reagent Co., LTD.), thiourea (CH_4N_2S, A.R., Shanghai Woke Biotechnology Co., LTD.), Ammonia water (H_5NO, A.R., Aladdin), Manganese(II) chloride tetrahydrate ($MnCl_2·4H_2O$ A.R., Sinopanax Chemical Reagent Co., LTD.), iron (III) chloride hexahydrate ($FeCl_3·6H_2O$, Sinopanax Chemical Reagent Co., LTD)ethanol (C_2H_5OH, A.R., Nanjing Chemical Reagents Co., LTD.), hydrochloric acid (HCl, A.R., Nanjing Chemical Reagents Co., LTD.), sodium hydroxide (NaOH, A.R., Sinophosphate Chemical Reagent Co., LTD.), potassium sulfate peroxide ($KHSO_5$, A.R., Macklin), sodium sulfate (Na_2SO_4, A.R., Sinophosphate Chemical Reagent Co., LTD.), sodium dihydrogen phosphate (NaH_2PO_4, A.R., Shanghai Yuanye Biotechnology Co., LTD.), sodium chloride (NaCl, A.R., Sinophosphate Chemical Reagents Co., LTD.), methanol (CH_3OH, A.R., Macklin), tert-butanol ($C_4H_{10}O$, A.R., Aladdin), L-histidine ($C_6H_9N_3O_2$, A.R.), tetracycline ($C_{22}H_{24}O_8N_2·HCl$, A.R., Bellingwell Technology Co., LTD., metronidazole ($C_6H_9N_3O_3$, A.R., Aladdin), methylene blue ($C_{16}H_{18}ClN_3S·3H_2O$, A.R.), levofloxacin ($C_{18}H_{20}FN_3O_4$, A.R.), malachite green ($C_{23}H_{25}ClN_2$, A.R.), Macklin), crystal violet ($C_{25}H_{30}N_3Cl·9H_2O$, A.R., Macklin), rhodamine B ($C_{28}H_{31}ClN_2O_3$, A.R., Macklin) were used in this experiment. Ultrapure water was used throughout all experiments.

1.2 Synthesis proceeding

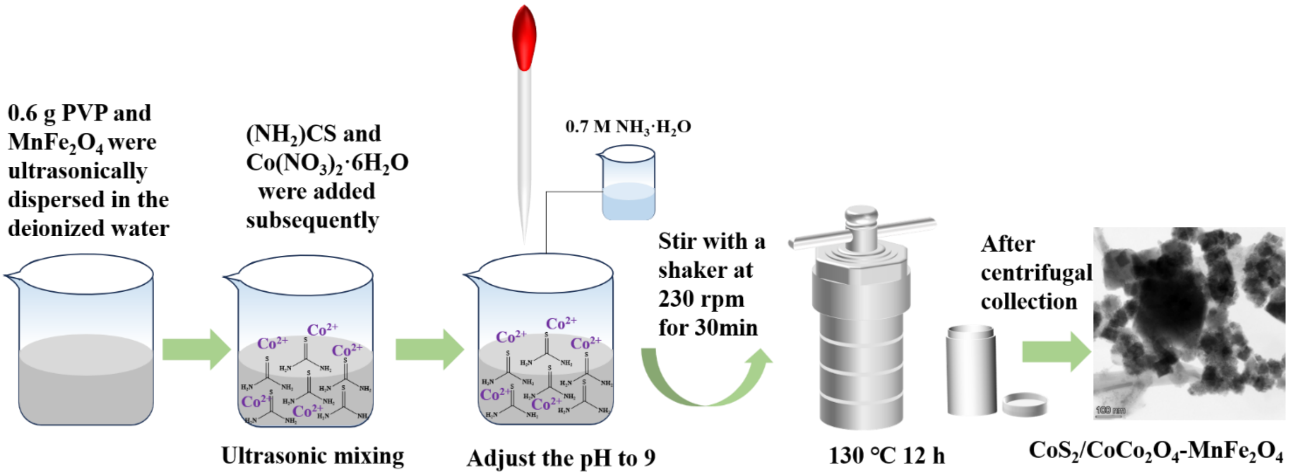

Figure S1. The schematic diagram of the synthetic route of $CoS_2/CoCo_2O_4$-$MnFe_2O_4$-x.

1.3 Analytical method

The concentration of pollutants in solution was measured by ultraviolet spectrometer, and the linear relationship between absorbance A of MNZ and concentration C (mg/L) is measured, as shown in Equation (2.1):

$$\text{MNZ: } A = 0.0528C - 0.01017 \qquad R^2 = 0.999 \qquad (2.1)$$

The linear relationship between absorbance (A) and concentration C (mg/L) of TC is measured, as shown in Equation (2.2):

$$\text{TC } A = 0.032C + 0.0065 \qquad R^2 = 0.999 \qquad (2.2)$$

The linear relationship between absorbance (A) and concentration C (mg/L) of LFX is measured, as shown in Equation (2.3):

$$\text{LFX: } A = 0.05973C + 0.09943 \qquad R^2 = 0.995 \qquad (2.3)$$

The linear relationship between absorbance (A) and concentration C (mg/L) of CV is measured, as shown in Equation (2.4):

$$\text{CV: } A = 0.09602C + 0.00682 \qquad R^2 = 0.999 \qquad (2.4)$$

The linear relationship between absorbance (A) and concentration C (mg/L) of RhB is measured, as shown in Equation (2.5):

$$\text{RhB: } A = 0.0268C + 0.0141 \qquad R^2 = 0.998 \tag{2.5}$$

The removal rate of pollutants is calculated according to Equation (2.6):

$$r = \frac{C_0 - C_t}{C_0} \times 100\% \tag{2.6}$$

Where, C_0 and C_t are the pollutant concentration at the initial time and time t respectively, mg/L.

In the degradation process of MB, it conforms to the pseudo-first-order kinetic model, as shown in Equation (2.10) [1] :

$$-\frac{dC_t}{dt} = k \times C_t \tag{2.10}$$

Where, k is the pseudo-first-order rate constant, expressed in min^{-1}.

1.4 Experimental method

Additionally, the effects of catalyst dose, PMS dose, initial concentration of TCH, and inorganic ions on the reaction were investigated. The experiment continues, by examining the effect of methanol (MeOH), tert-Butanol (tert-Buoh), trichloromethane ($CHCl_3$) and L-Histidine on the removal performance, determine the type of radical involved. Moreover, cyclic tests were conducted to evaluate the reusability and stability of the catalyst. After each operation, the used catalyst is collected with magnet, washed with ultra-pure water and dried, and then no other treatment is done to continue the degradation experiment. The experimental process is the same as the above operation of degradation experiment. The ions (Fe, Co and Mn) leached from the catalyst surface were detected by ICP-MS in the cyclic test. Finally, the possible activation mechanism and active components of PMS are described in detail. It is worth noting that the experiment was conducted three times and the results were expressed as averages.

1.5 Representational means

The surface morphology of the catalyst was observed by scanning electron microscopy (SEM, Quant 250FEG, FEI Corporation) and transmission electron microscopy (TEM, Talos F200X, FEI Corporation). The crystal structure and composition were analyzed by X-ray diffractometer (XRD, Bruker D8 Advance, Bruker, Germany). The test conditions were as follows: the target was copper, the scanning range was 20~90º, and the scanning speed was 2 °/min. The composition and state of the elements on the surface of the sample were analyzed by X-ray photoelectron spectrometer (XPS, PHI QuanteraII, Ulvac-Phi, Japan) under the test condition of Al-kα X-ray. Chemical bonding and identification of chemical species were studied by Fourier infrared spectrometer (TFIR, NICOLETIS10, Thermo Fisher Technology). The test conditions were: mid-infrared KBr beam splitter, DTGS detector, KBr window, scanning range of 4000~500 cm^{-1}. Oxygen defects in the material were detected by paramagnetic resonance spectroscopy (EPR, Bruker A300, Bruker GMBH). The leaching content of metal elements in materials was detected by inductively coupled plasma mass spectrometer (ICP-MS, i-CAPQ, ThermoFisher). The magnetic properties of different materials are tested by superconducting quantum magnetometer (VSM, SQUID-VSM, SI).

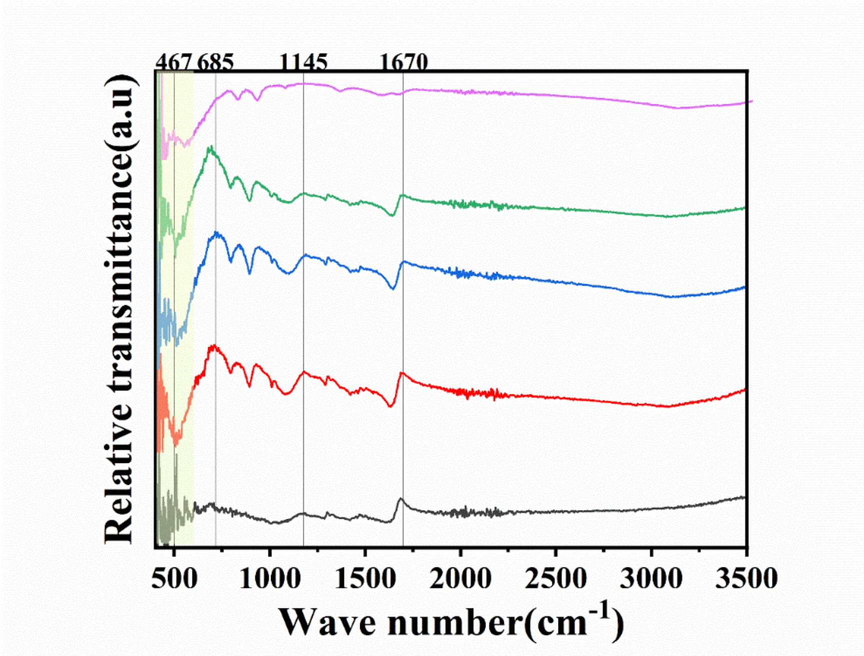

Figure S2. FT-IR spectra of $CoS_2/CoCo_2O_4$, $MnFe_2O_4$ and $CoS_2/CoCo_2O_4$-$MnFe_2O_4$-x samples.

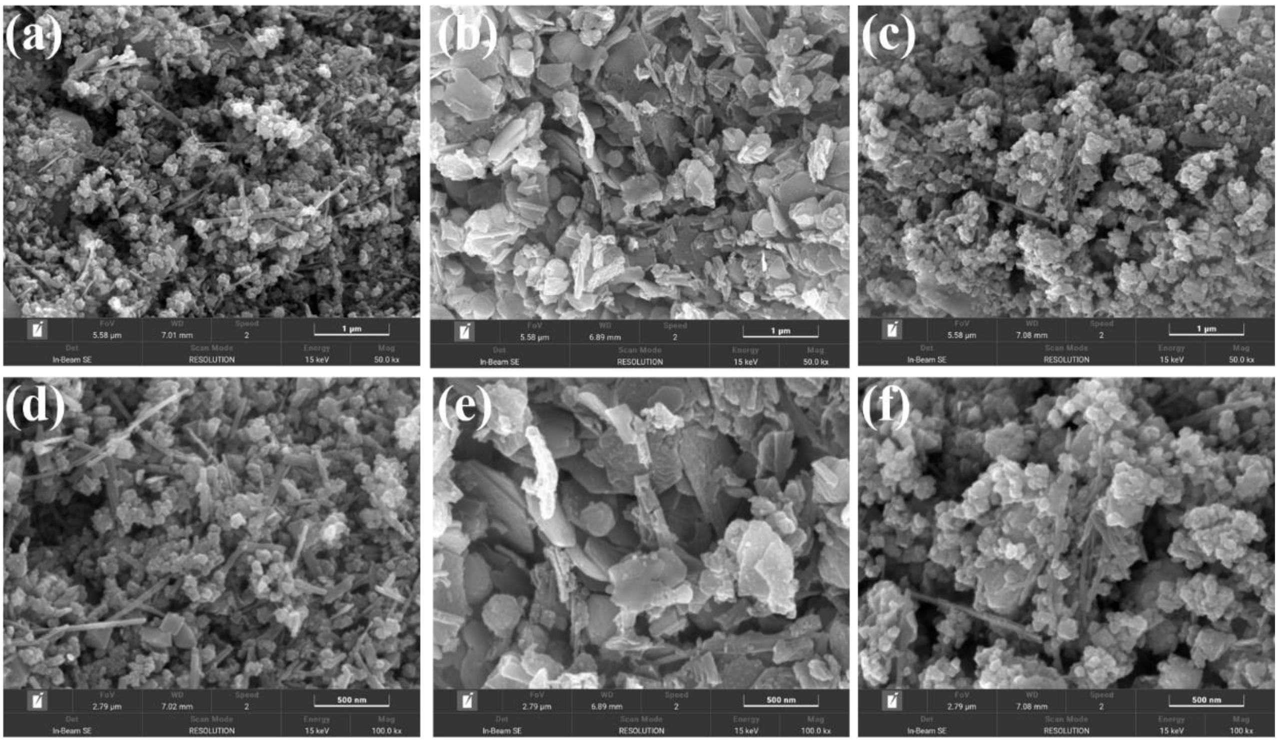

Figure S3. (a) SEM image of $MnFe_2O_4$ at 50 kx, (b) SEM image of $CoS_2/CoCo_2O_4$ at 50 kx, (c) SEM image of $CoS_2/CoCo_2O_4$-$MnFe_2O_4$ at 50 kx; (d) SEM image of $MnFe_2O_4$ at 100 kx, (e) SEM image of $CoS_2/CoCo_2O_4$ at 100 kx, (f) SEM image of $CoS_2/CoCo_2O_4$-$MnFe_2O_4$ at 100 kx.

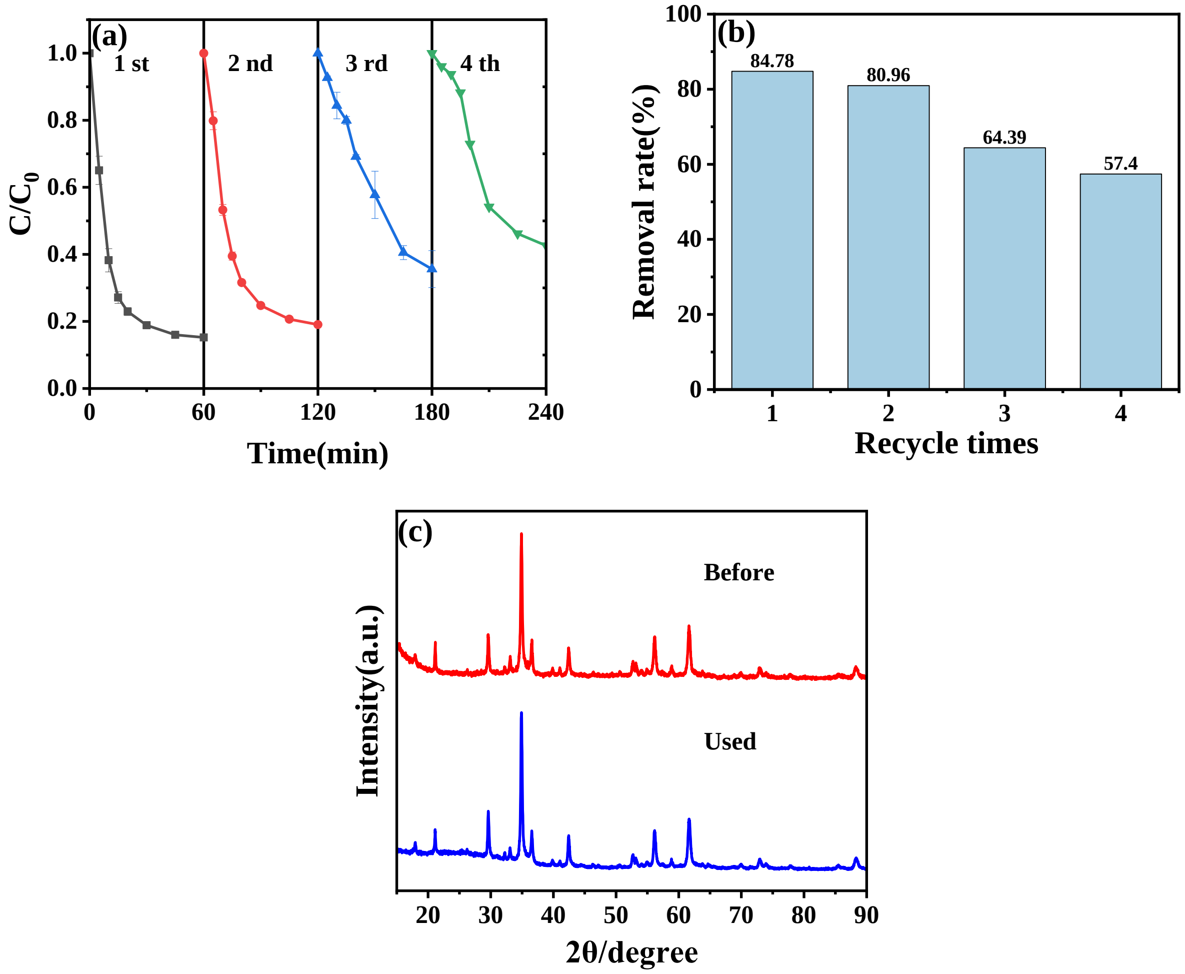

Figure S4. (a) Reusability test for $CoS_2/CoCo_2O_4$-$MnFe_2O_4$-2 Experimental conditions: [catalyst] = 100 mg/L, $[PMS]_0$ = 1 mM, $[TC]_0$= 20 mg/L, pH = 7, T = 288 K; (b) Bar chart of removal rate corresponding to (a); (c) XRD patterns of before and used $CoS_2/CoCo_2O_4$-$MnFe_2O_4$-2.

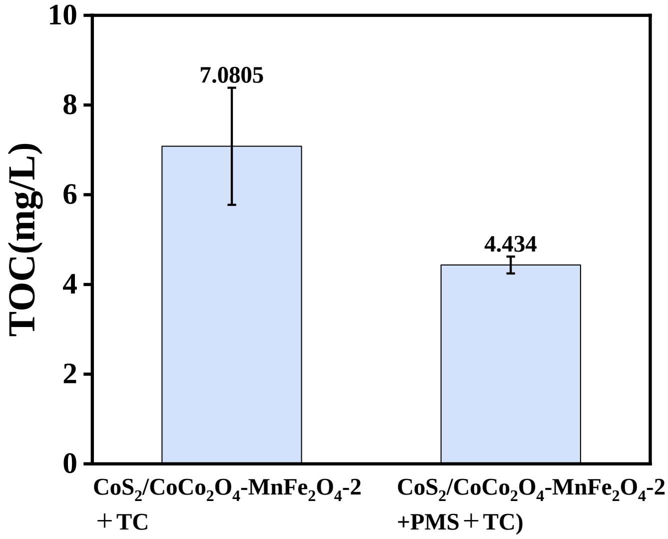

Figure S5. Bar graph of TOC in different systems.

Table S1. Possible degradation intermediates of TC in the $CoS_2/CoCo_2O_4-MnFe_2O_4-2/PMS$ system.

Products	Retention time (min)	Mass (m/z)	Supposed Structure
TC	9.23	445	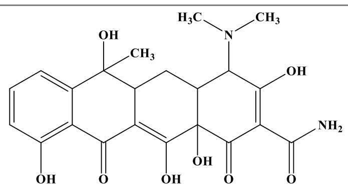
P1	7.28	397	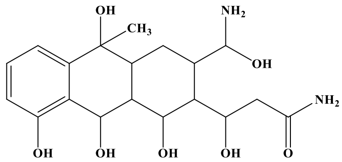
P2	1.22	297	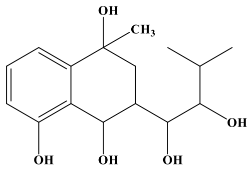
P3	1.17	195	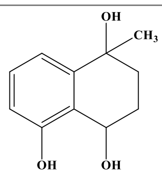
P4	0.80	431	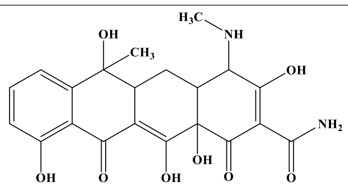

P5	0.82	413	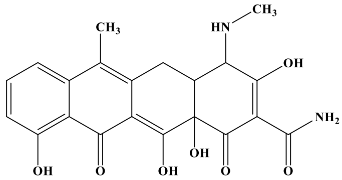
P6	7.96	332	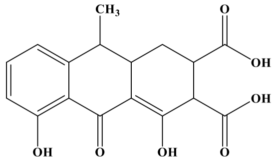
P7	0.84	289	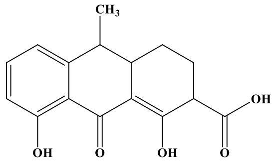
P8	6.62	404	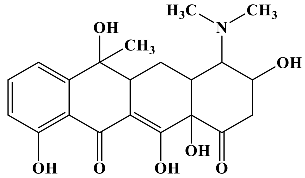
P9	9.24	341	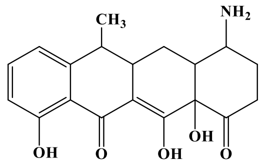
P10	0.61	301	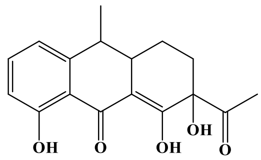
P11	6.16	217	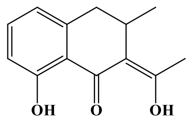
P12	4.34	172	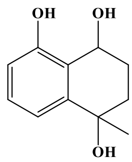
P13	5.92	200	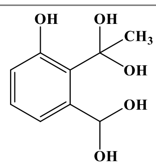
P14	6.33	341	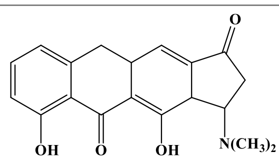
P15	6.88	270	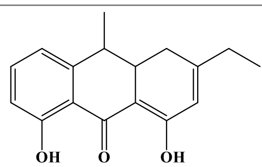

P16	5.31	183	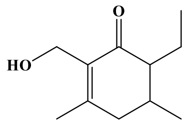
P17	4.34	155	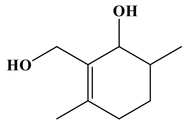
P18	1.22	149	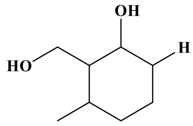
P19	0.67	226	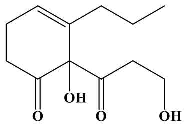
P20	4.85	130	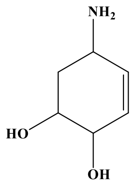
P21	4.41	94	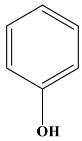
P22	6.45	74	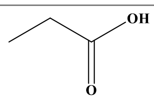
P23	3.94	60	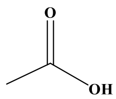

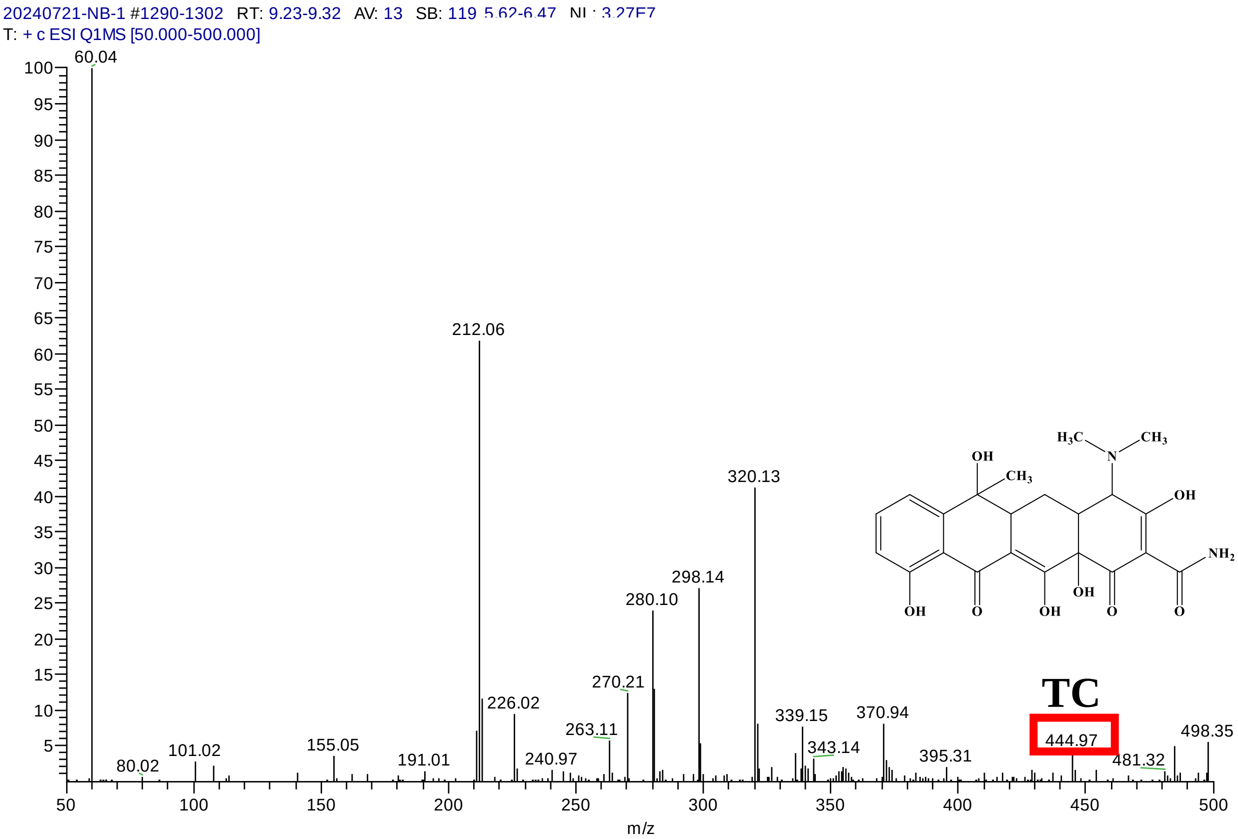
20240721-NB-1 #1290-1302 RT: 9.23-9.32 AV: 13 SB: 119 5.62-6.47 NL: 3.27E7
T: + c ESI Q1MS [50.000-500.000]
60.04
212.06
320.13
298.14
280.10
270.21
226.02
263.11
339.15
370.94
343.14
101.02
155.05
80.02
191.01
240.97
395.31
444.97
481.32
498.35
TC
H3C
CH3
N
OH
CH3
OH
NH2
OH
O
OH
OH
O
O
m/z

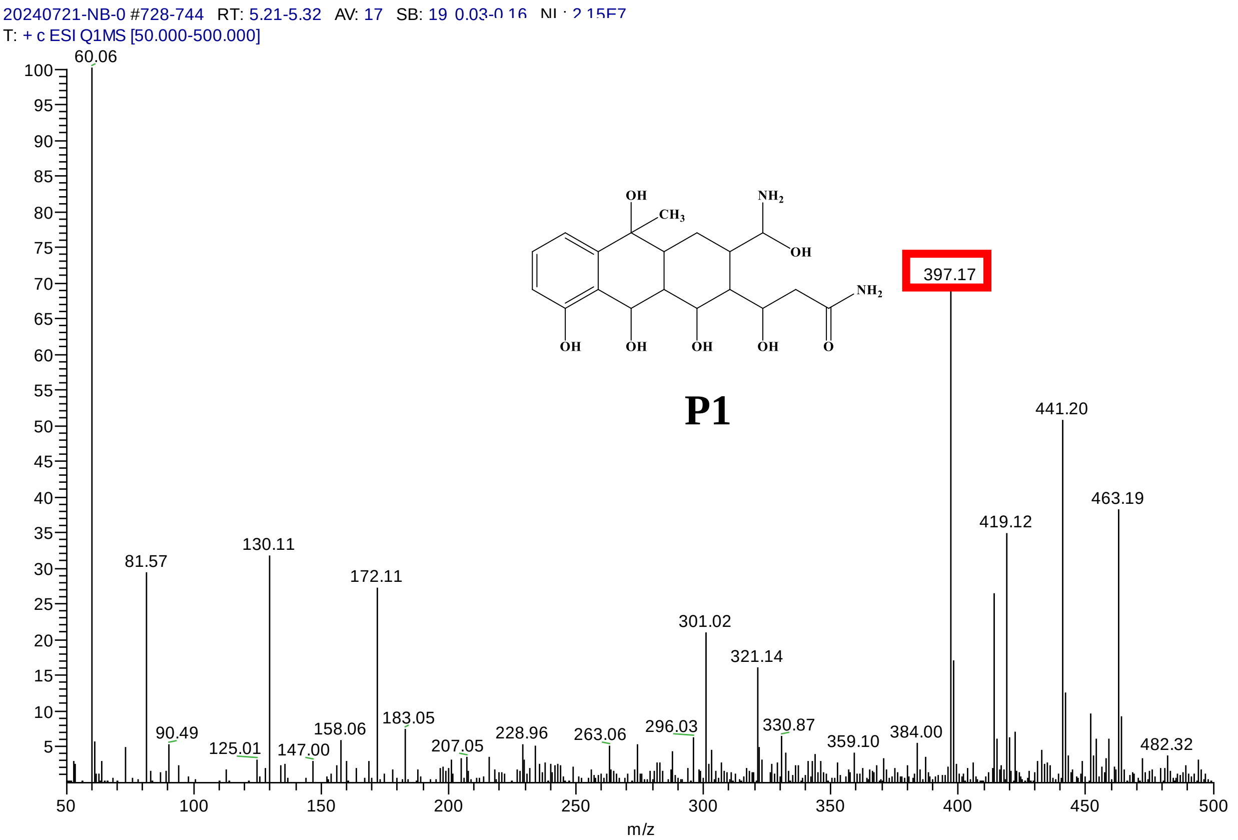
20240721-NB-0 #728-744 RT: 5.21-5.32 AV: 17 SB: 19 0.03-0.16 NL: 2.15E7
T: + c ESI Q1MS [50.000-500.000]
60.06
397.17
441.20
463.19
419.12
130.11
81.57
172.11
301.02
321.14
183.05
90.49
125.01
147.00
158.06
207.05
228.96
263.06
296.03
330.87
359.10
384.00
482.32
P1
OH
CH3
NH2
OH
NH2
OH
OH
OH
OH
O
m/z

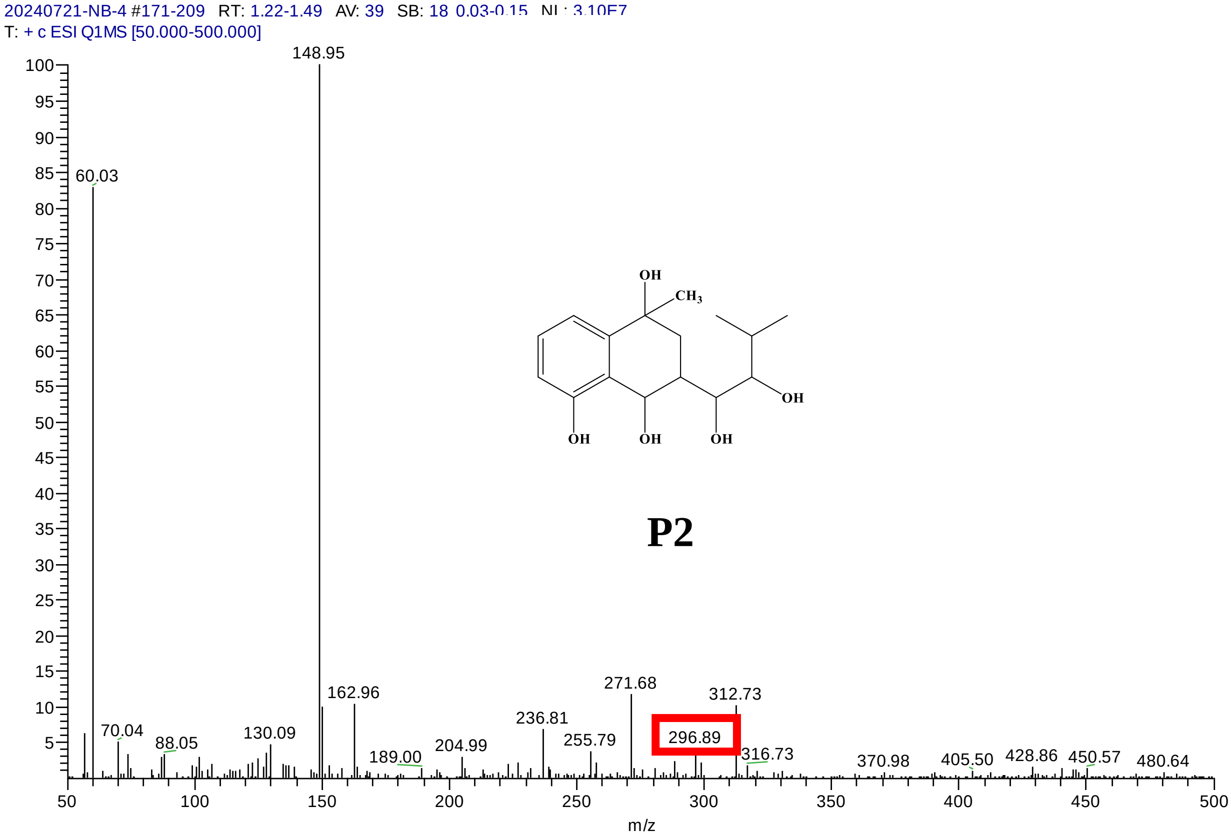
20240721-NB-4 #171-209 RT: 1.22-1.49 AV: 39 SB: 18 0.03-0.15 NL: 3.10E7
T: + c ESI Q1MS [50.000-500.000]
148.95
60.03
70.04
88.05
130.09
162.96
189.00
204.99
236.81
255.79
271.68
296.89
312.73
316.73
370.98
405.50
428.86
450.57
480.64
OH
CH3
OH
OH
OH
OH
P2
m/z

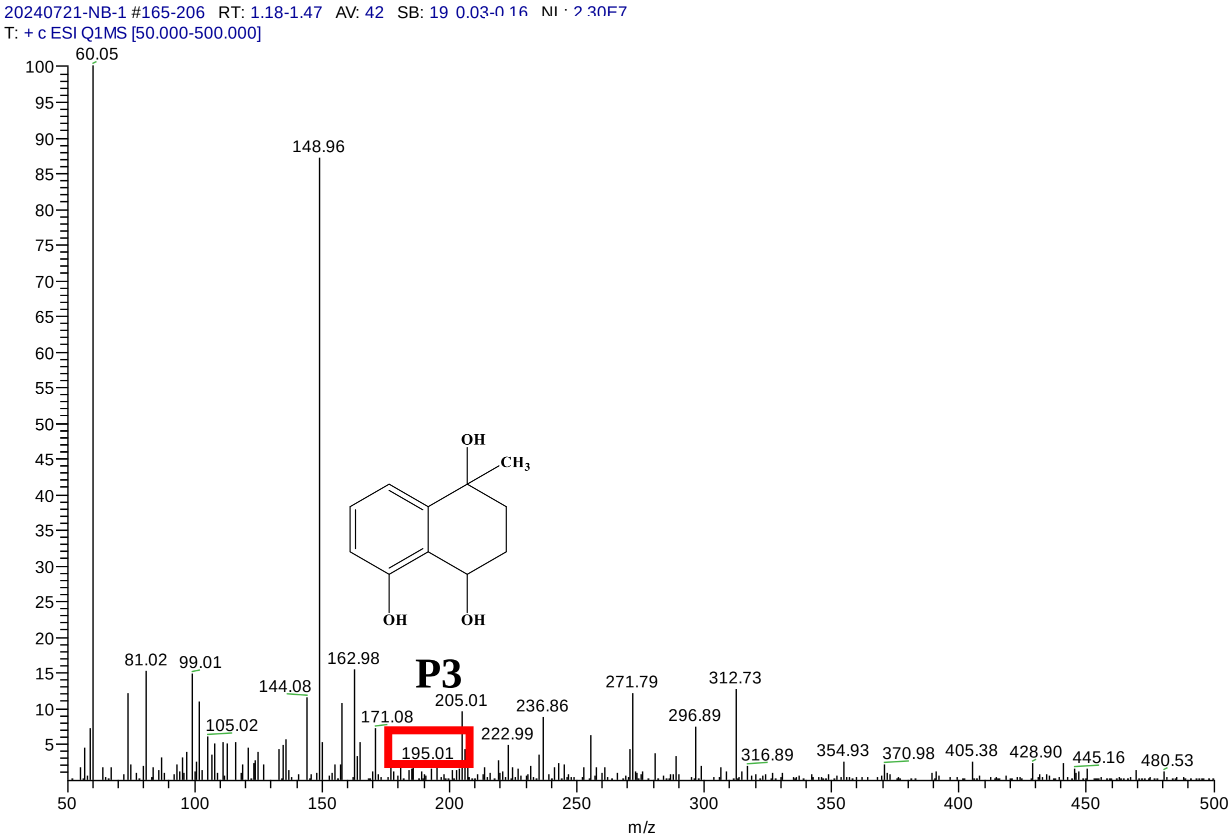
20240721-NB-1 #165-206 RT: 1.18-1.47 AV: 42 SB: 19 0.03-0.16 NL: 2.30E7
T: + c ESI Q1MS [50.000-500.000]
60.05
148.96
81.02
99.01
105.02
144.08
162.98
171.08
195.01
205.01
222.99
236.86
271.79
296.89
312.73
316.89
354.93
370.98
405.38
428.90
445.16
480.53
OH
CH3
OH
OH
P3
m/z

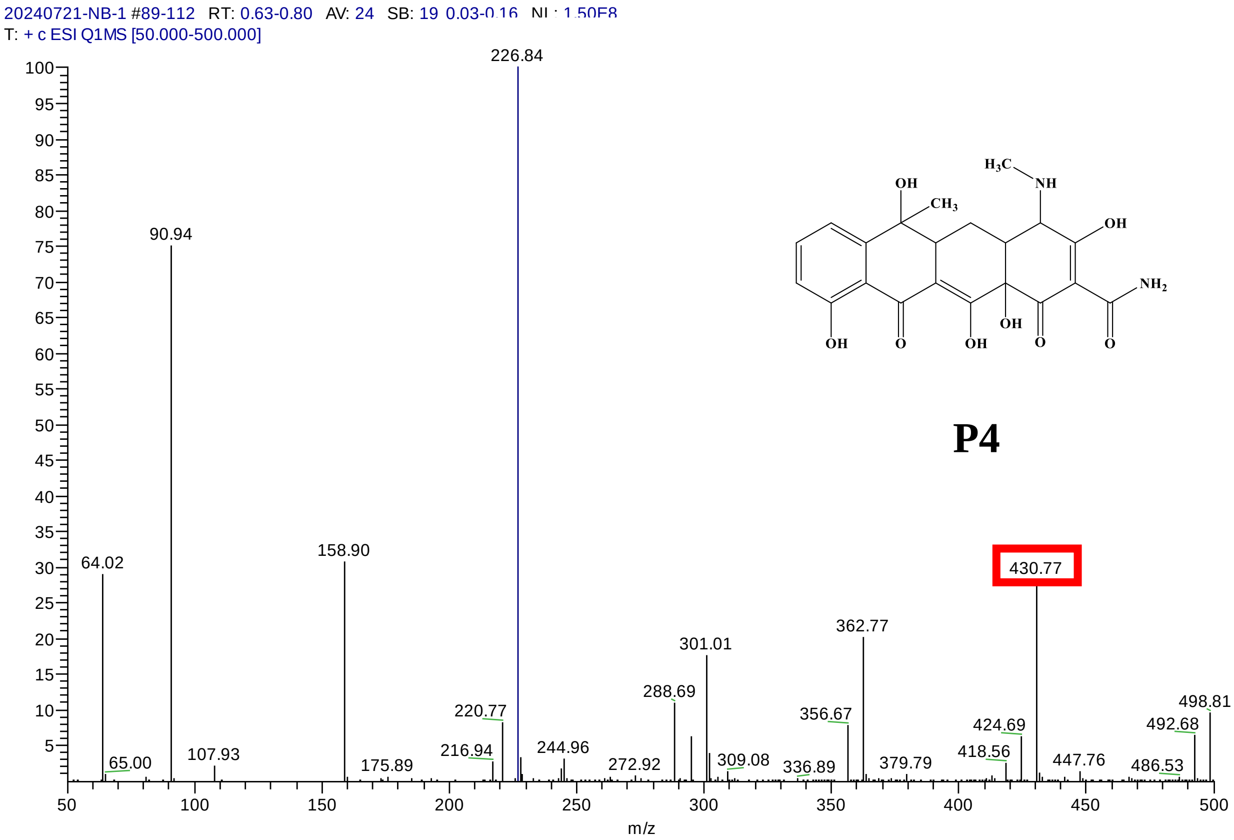
20240721-NB-1 #89-112 RT: 0.63-0.80 AV: 24 SB: 19 0.03-0.16 NL: 1.50E8
T: + c ESI Q1MS [50.000-500.000]
226.84
90.94
64.02
158.90
430.77
362.77
301.01
288.69
220.77
356.67
498.81
424.69
492.68
216.94
244.96
418.56
107.93
309.08
65.00
175.89
272.92
336.89
379.79
447.76
486.53
m/z
P4

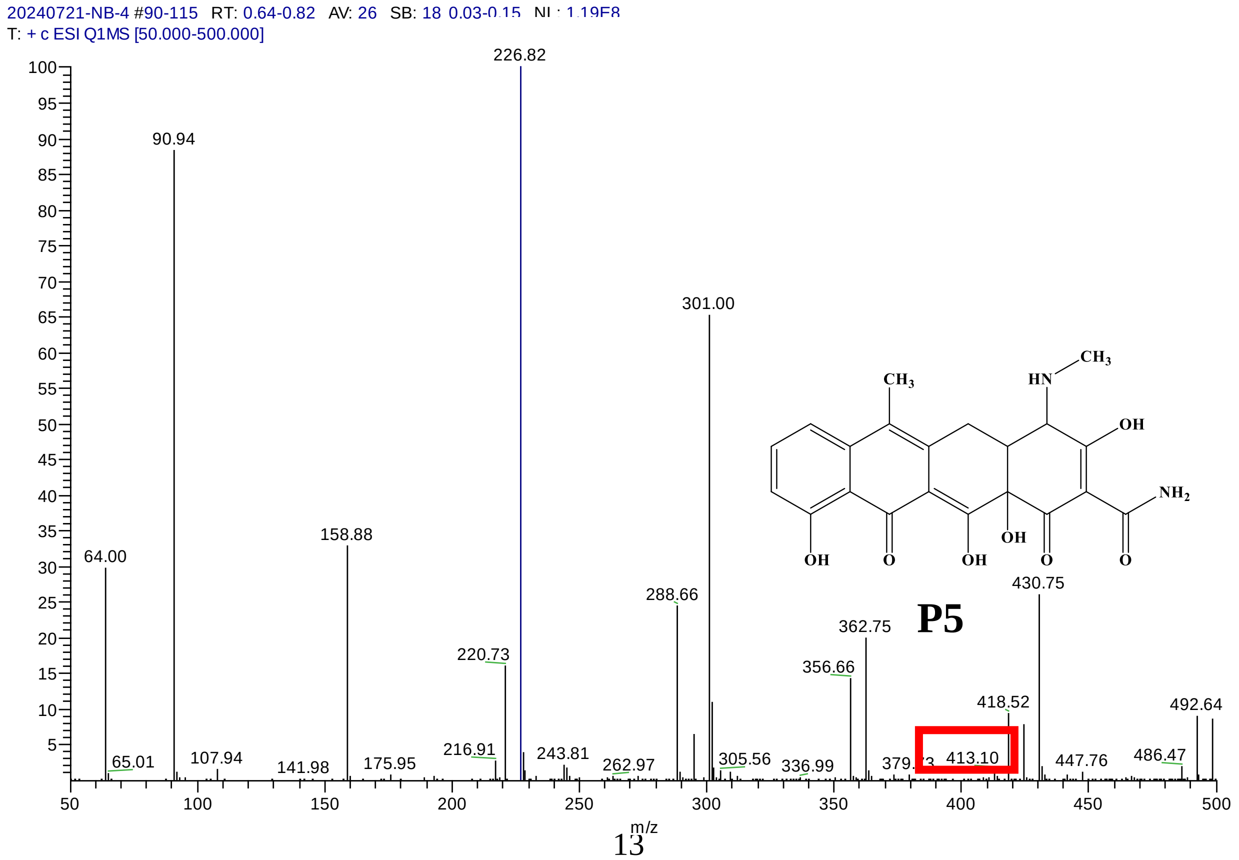
20240721-NB-4 #90-115 RT: 0.64-0.82 AV: 26 SB: 18 0.03-0.15 NL: 1.19E8
T: + c ESI Q1MS [50.000-500.000]
226.82
90.94
301.00
158.88
64.00
430.75
288.66
362.75
220.73
356.66
418.52
492.64
216.91
243.81
107.94
65.01
141.98
175.95
262.97
305.56
336.99
413.10
447.76
486.47
m/z
P5

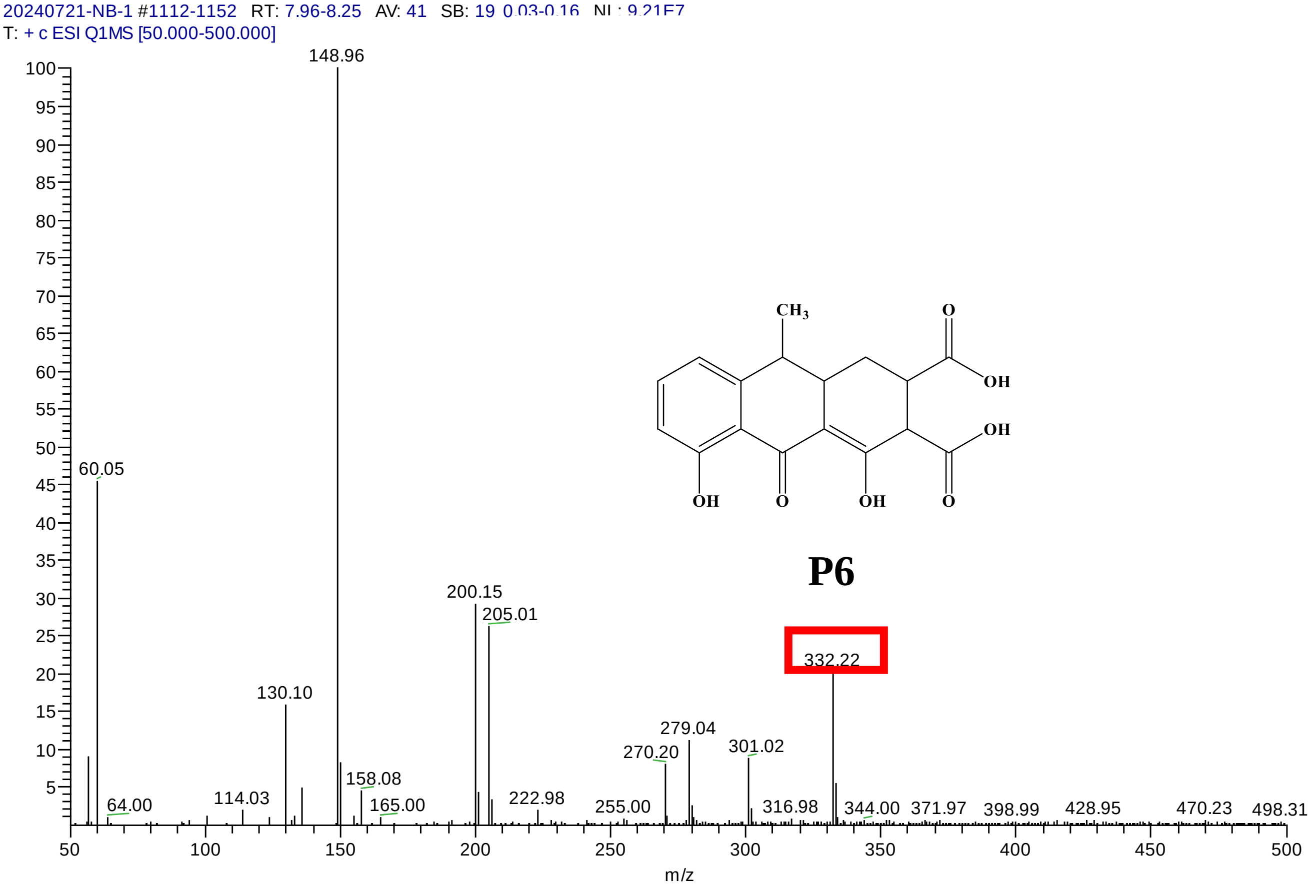
20240721-NB-1 #1112-1152 RT: 7.96-8.25 AV: 41 SB: 19 0.03-0.16 NL: 9.21E7
T: + c ESI Q1MS [50.000-500.000]
148.96
60.05
64.00
114.03
130.10
158.08
165.00
200.15
205.01
222.98
255.00
270.20
279.04
301.02
316.98
332.22
344.00
371.97
398.99
428.95
470.23
498.31
m/z
P6

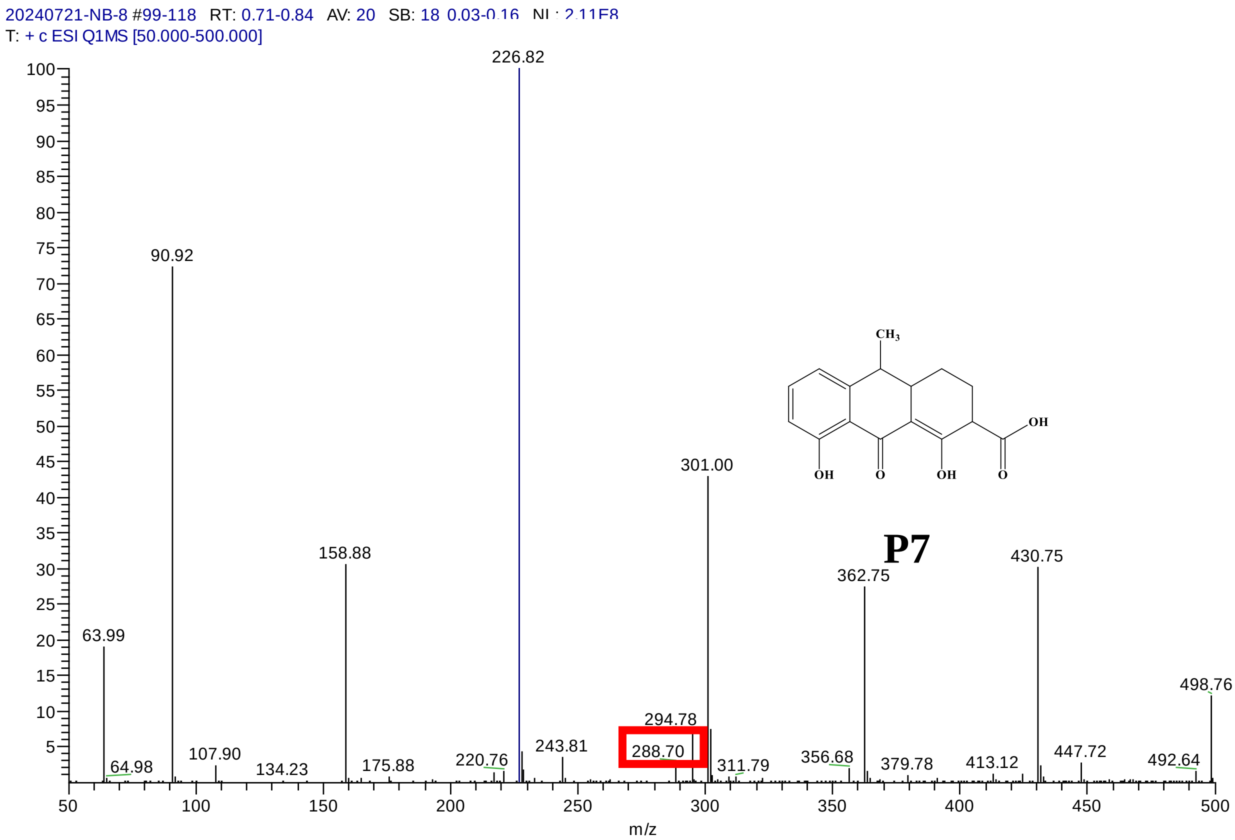
20240721-NB-8 #99-118 RT: 0.71-0.84 AV: 20 SB: 18 0.03-0.16 NL: 2.11E8
T: + c ESI Q1MS [50.000-500.000]
226.82
90.92
63.99
64.98
107.90
134.23
158.88
175.88
220.76
243.81
288.70
294.78
301.00
311.79
356.68
362.75
379.78
413.12
430.75
447.72
492.64
498.76
m/z
P7

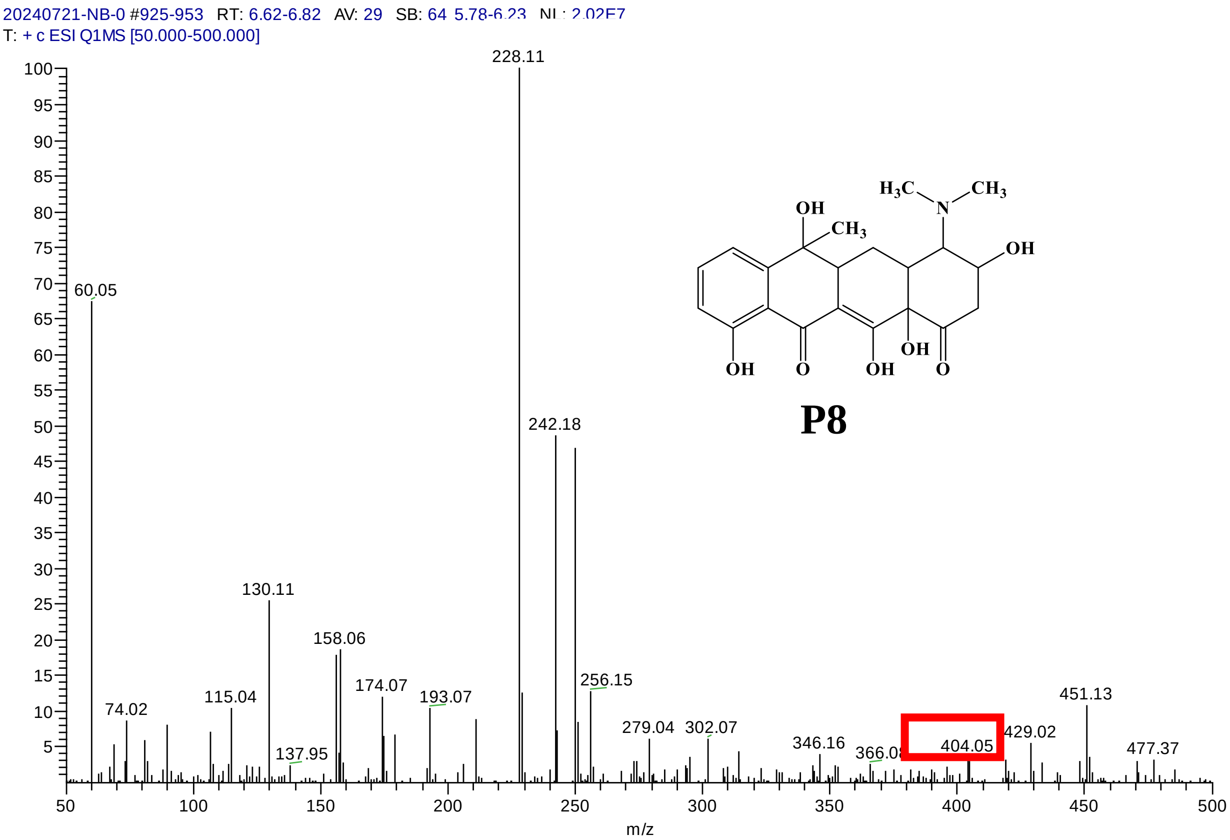

20240721-NB-0 #925-953 RT: 6.62-6.82 AV: 29 SB: 64 5.78-6.23 NL: 2.02E7
T: + c ESI Q1MS [50.000-500.000]
228.11
60.05
242.18
130.11
158.06
174.07
193.07
256.15
115.04
74.02
137.95
279.04
302.07
346.16
366.08
404.05
429.02
451.13
477.37
m/z
P8

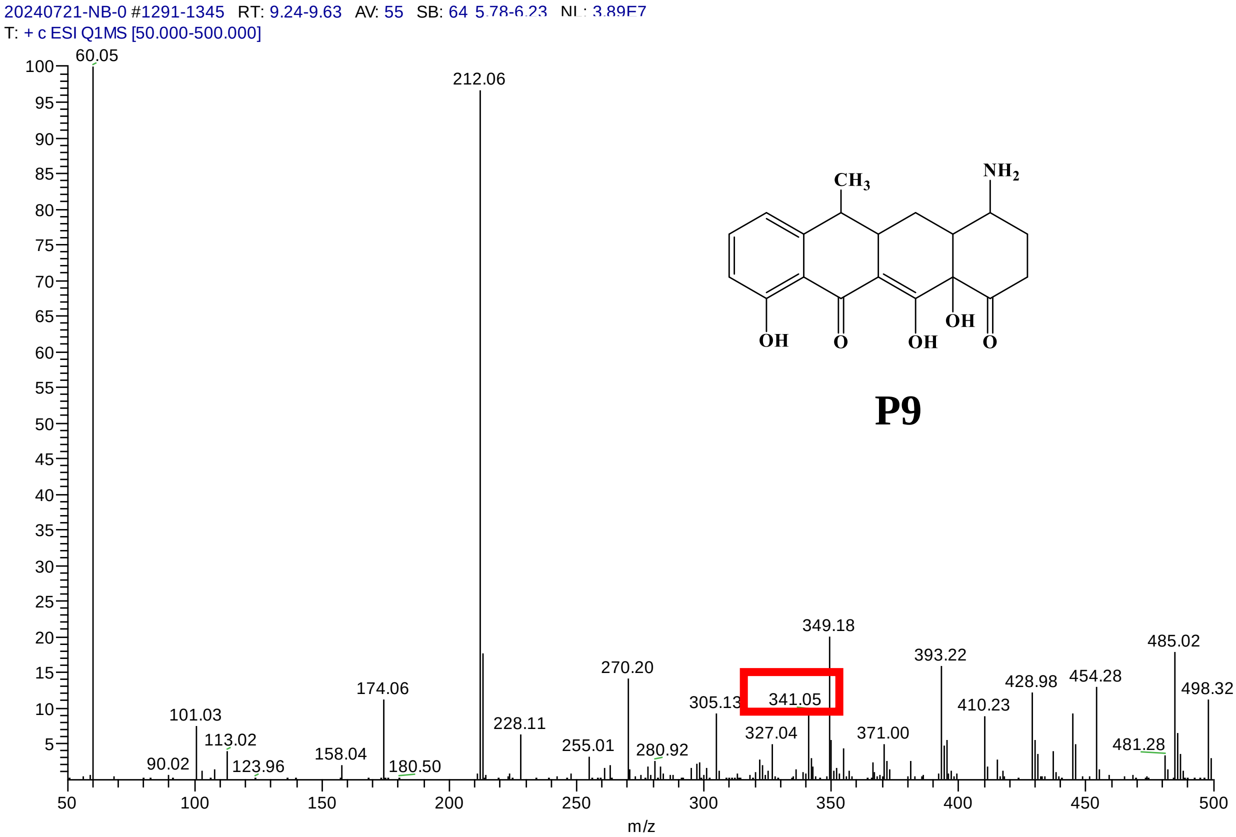

20240721-NB-0 #1291-1345 RT: 9.24-9.63 AV: 55 SB: 64 5.78-6.23 NL: 3.89E7
T: + c ESI Q1MS [50.000-500.000]
60.05
212.06
349.18
393.22
485.02
428.98
454.28
498.32
270.20
174.06
305.13
341.05
410.23
101.03
228.11
327.04
371.00
113.02
255.01
280.92
481.28
90.02
123.96
158.04
180.50
m/z
P9

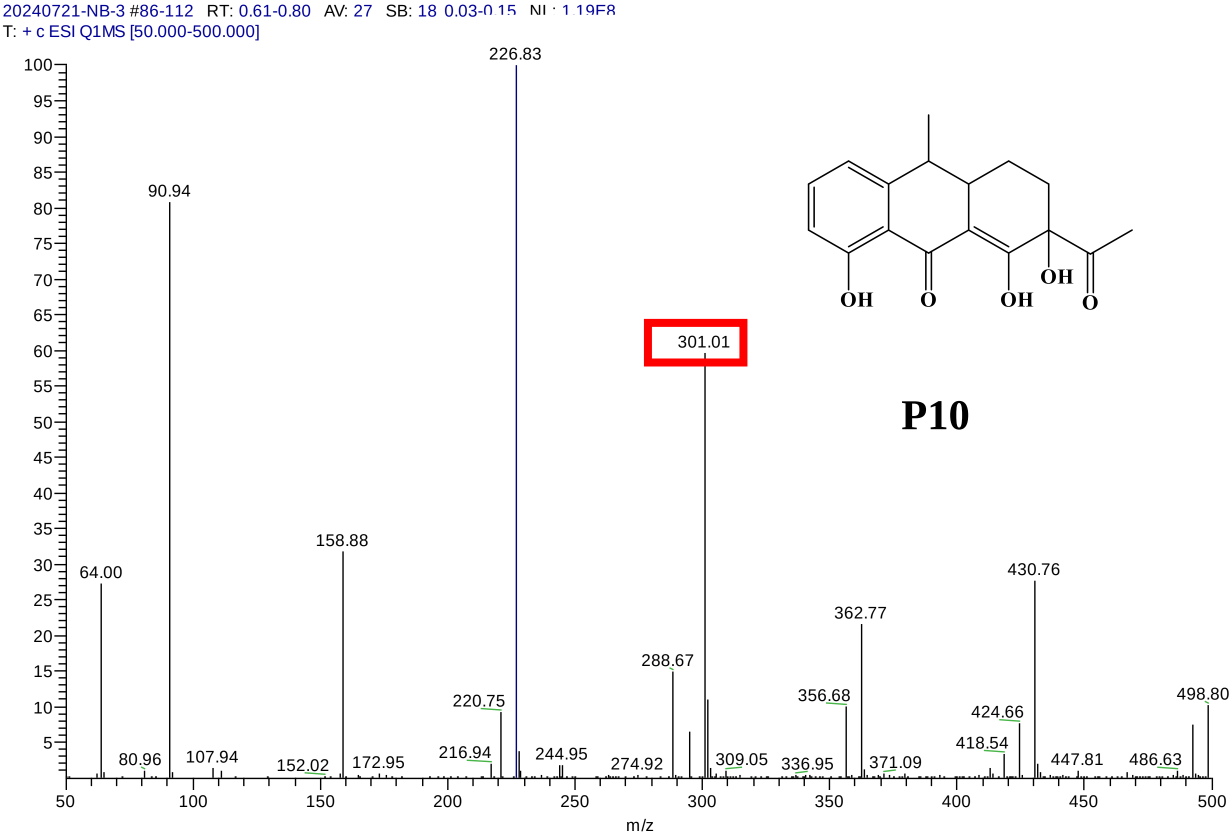
20240721-NB-3 #86-112 RT: 0.61-0.80 AV: 27 SB: 18 0.03-0.15 NL: 1.19E8
T: + c ESI Q1MS [50.000-500.000]
226.83
90.94
158.88
64.00
301.01
430.76
362.77
288.67
220.75
356.68
498.80
424.66
418.54
216.94
244.95
80.96
107.94
152.02
172.95
274.92
309.05
336.95
371.09
447.81
486.63
OH
O
OH
OH
O
P10
m/z

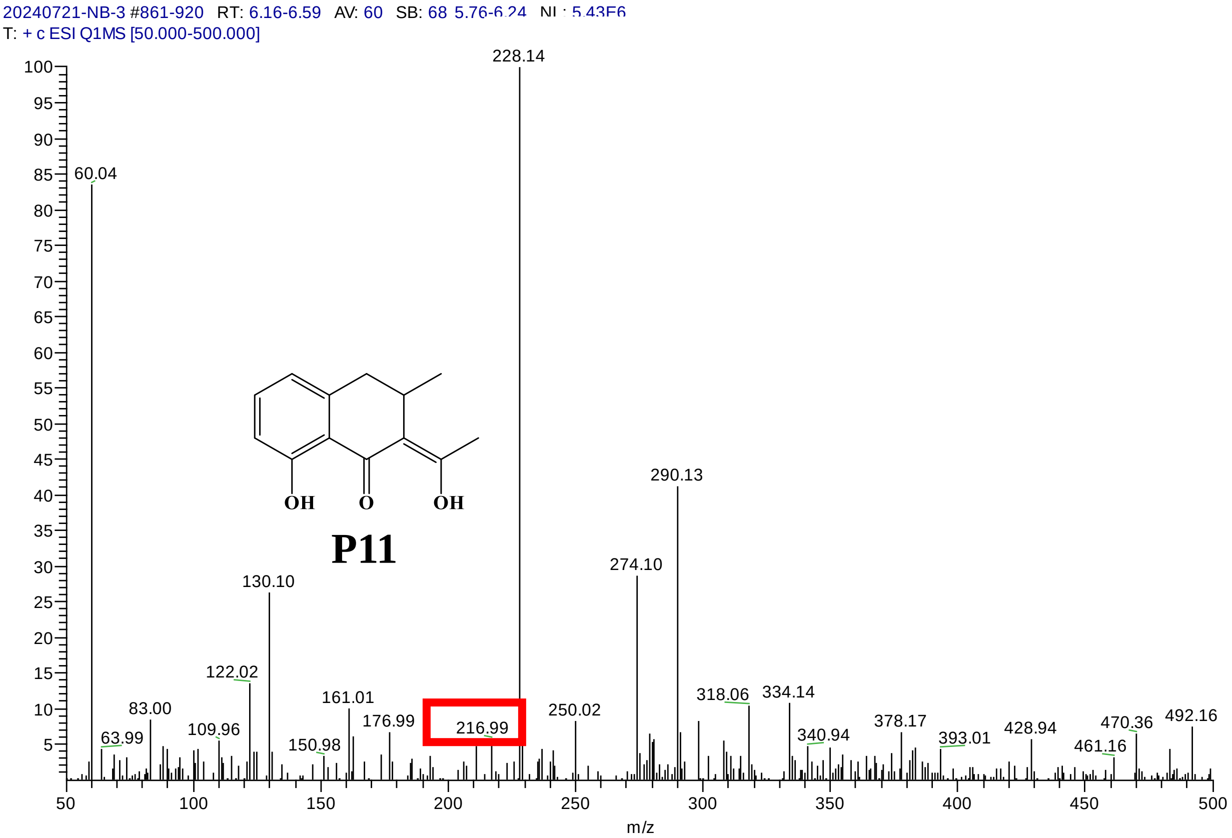
20240721-NB-3 #861-920 RT: 6.16-6.59 AV: 60 SB: 68 5.76-6.24 NL: 5.43E6
T: + c ESI Q1MS [50.000-500.000]
228.14
60.04
OH
O
OH
P11
290.13
274.10
130.10
122.02
83.00
161.01
176.99
216.99
250.02
318.06
334.14
63.99
109.96
150.98
340.94
378.17
393.01
428.94
461.16
470.36
492.16
m/z

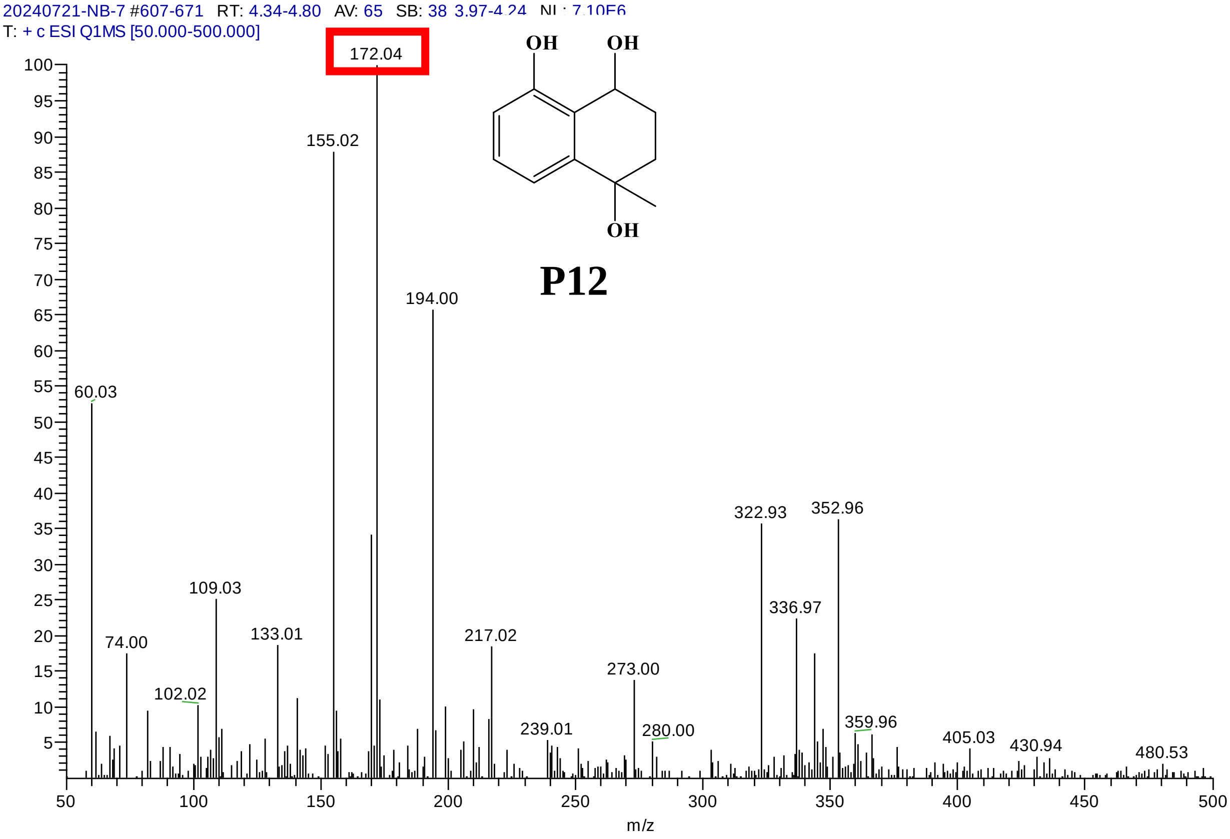

20240721-NB-7 #607-671 RT: 4.34-4.80 AV: 65 SB: 38 3.97-4.24 NL: 7.10E6
T: + c ESI Q1MS [50.000-500.000]
172.04
155.02
194.00
60.03
74.00
102.02
109.03
133.01
217.02
239.01
273.00
280.00
322.93
336.97
352.96
359.96
405.03
430.94
480.53
m/z
OH
OH
OH
P12

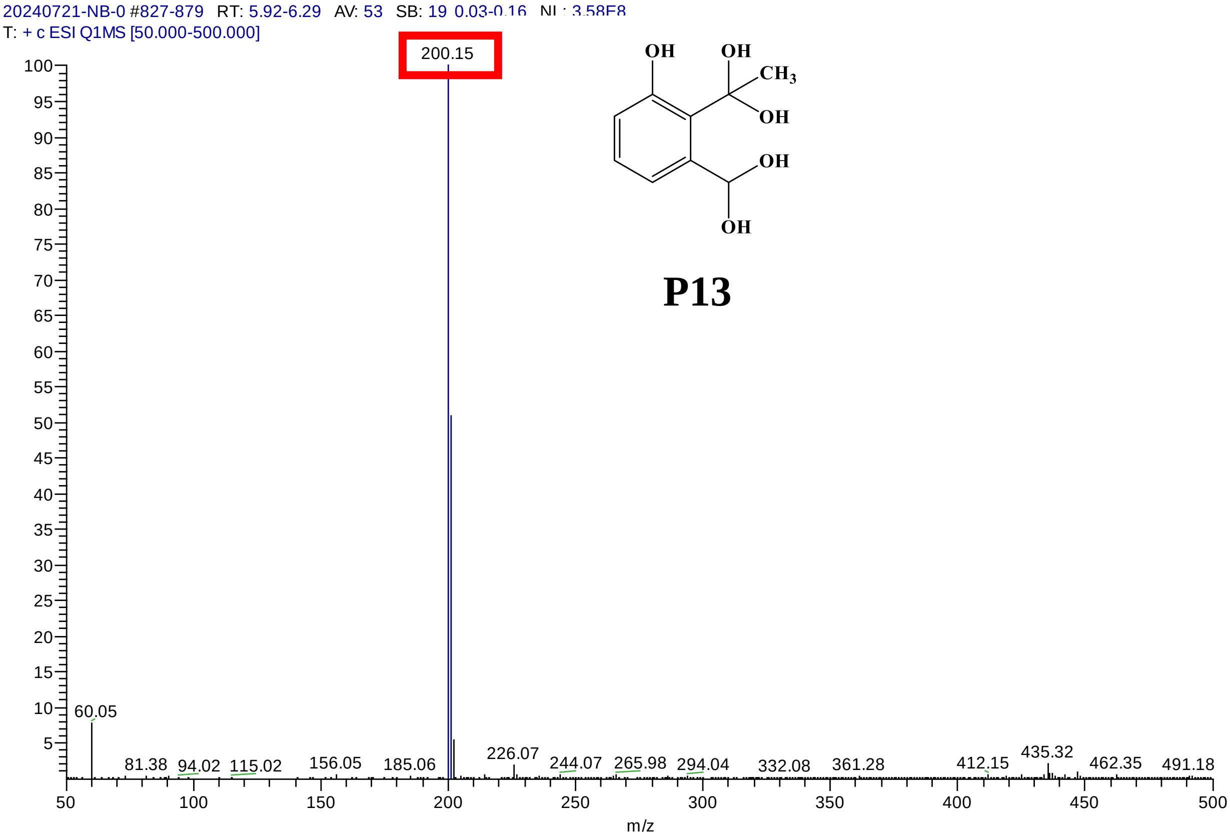

20240721-NB-0 #827-879 RT: 5.92-6.29 AV: 53 SB: 19 0.03-0.16 NL: 3.58E8
T: + c ESI Q1MS [50.000-500.000]
200.15
60.05
81.38
94.02
115.02
156.05
185.06
226.07
244.07
265.98
294.04
332.08
361.28
412.15
435.32
462.35
491.18
m/z
OH
OH
CH3
OH
OH
OH
P13

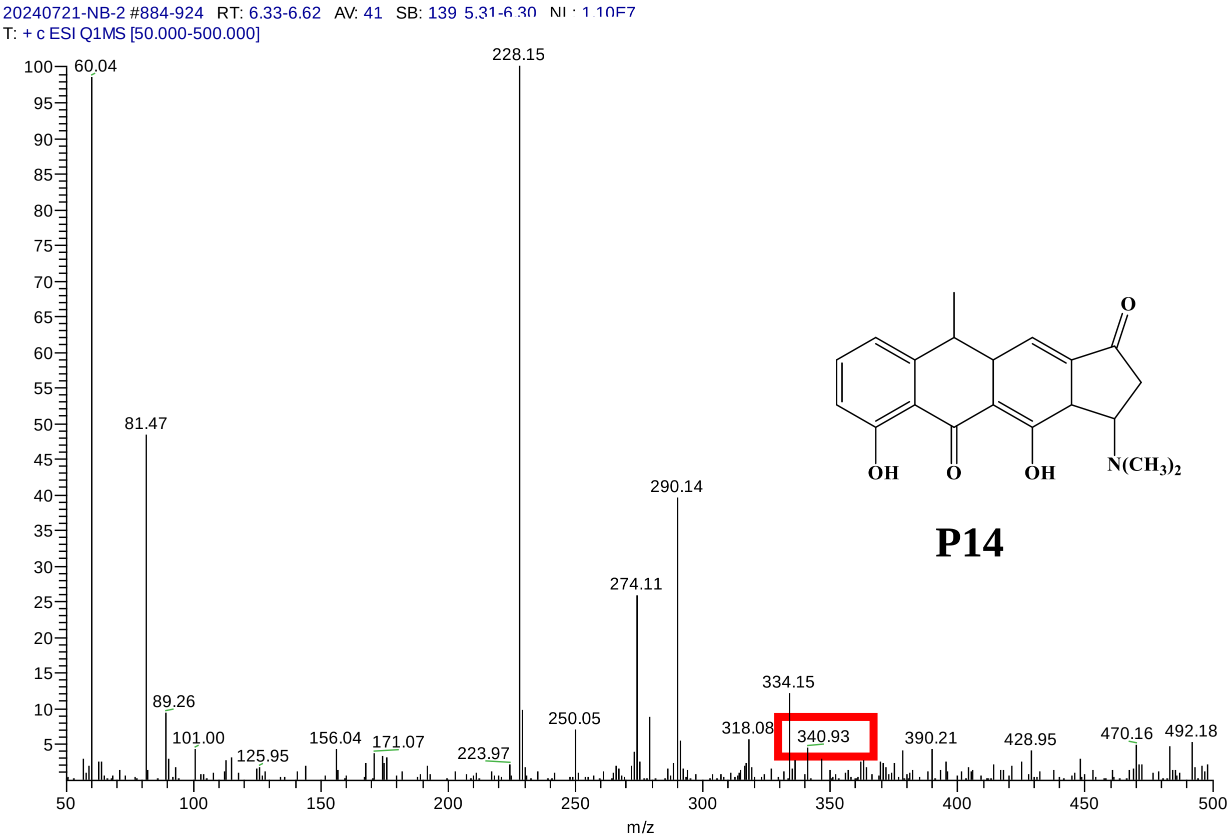
20240721-NB-2 #884-924 RT: 6.33-6.62 AV: 41 SB: 139 5.31-6.30 NL: 1.10E7
T: + c ESI Q1MS [50.000-500.000]
60.04
228.15
81.47
290.14
274.11
334.15
89.26
318.08
340.93
101.00
156.04
171.07
250.05
390.21
428.95
470.16
492.18
125.95
223.97
m/z
OH
O
OH
O
N(CH3)2

P14

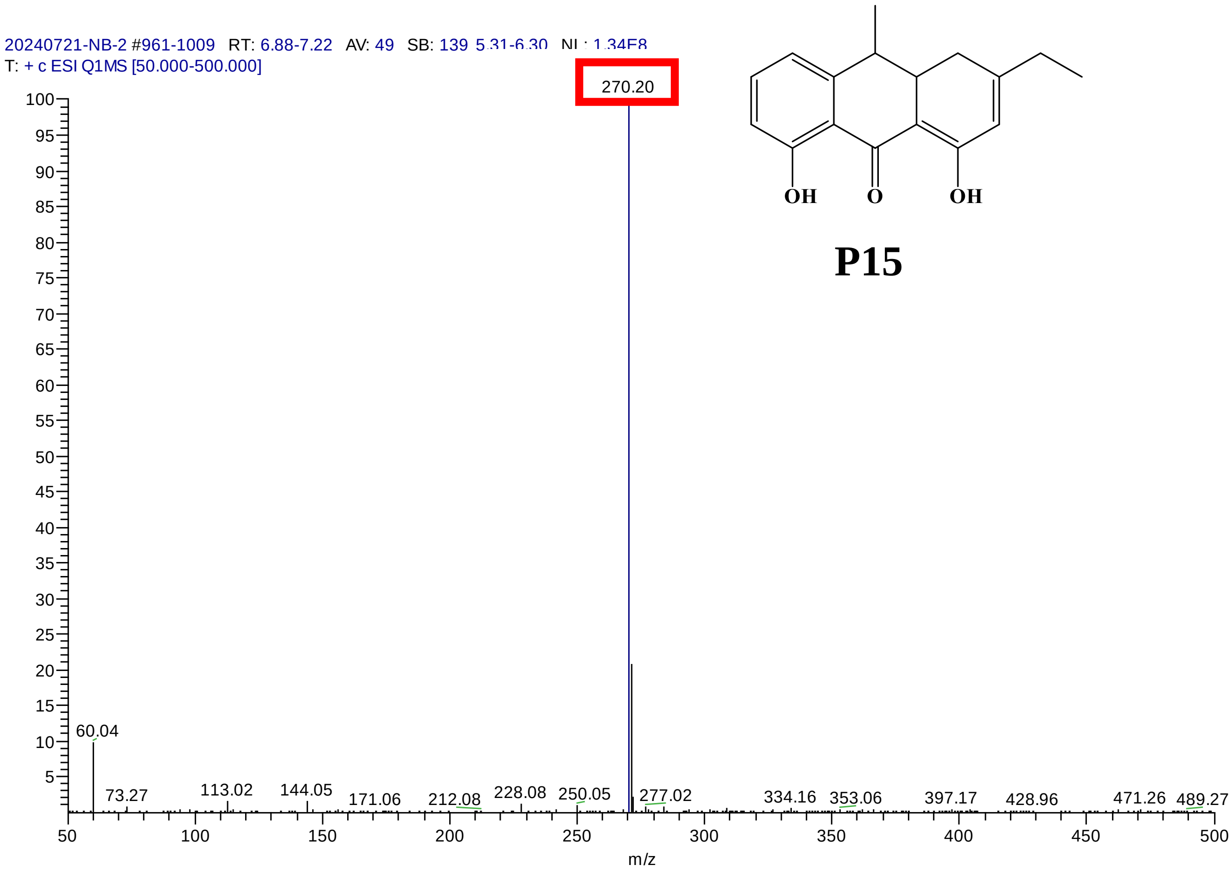
20240721-NB-2 #961-1009 RT: 6.88-7.22 AV: 49 SB: 139 5.31-6.30 NL: 1.34E8
T: + c ESI Q1MS [50.000-500.000]
270.20
60.04
73.27
113.02
144.05
171.06
212.08
228.08
250.05
277.02
334.16
353.06
397.17
428.96
471.26
489.27
m/z
OH
O
OH

P15

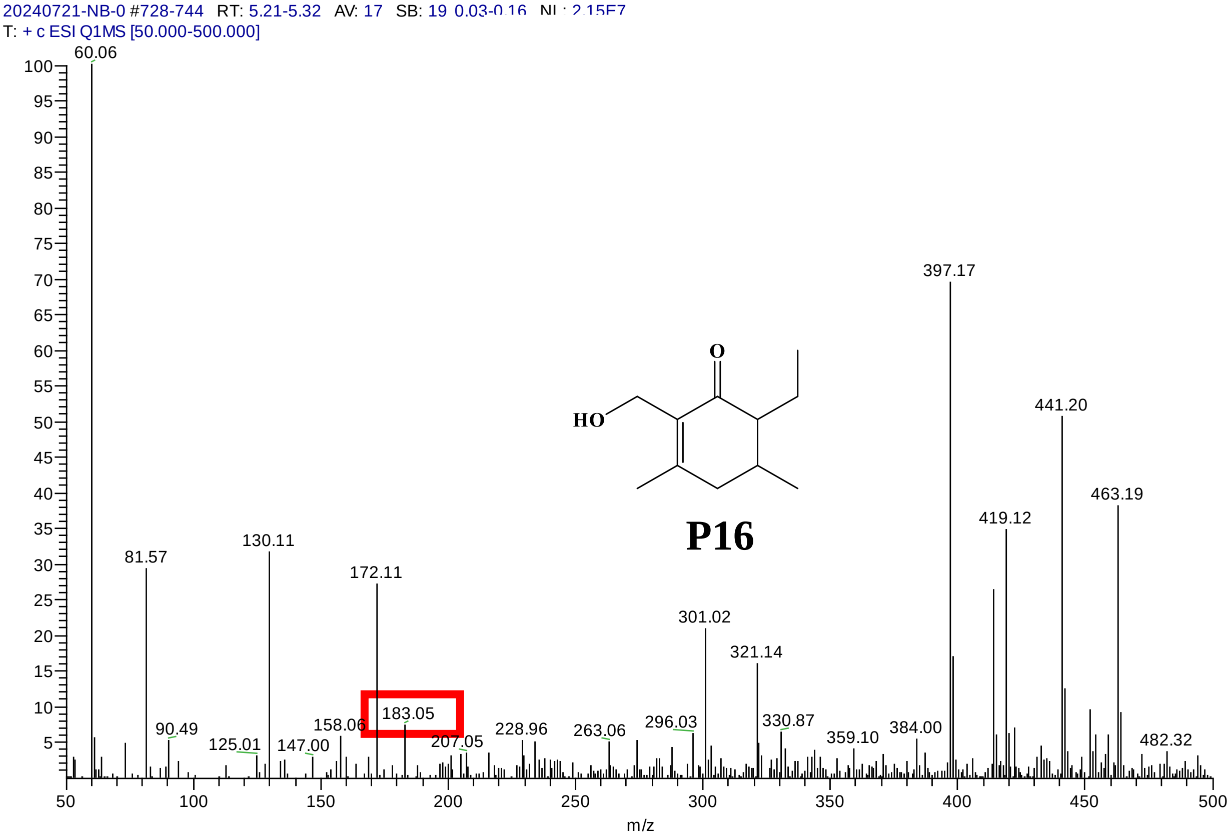
20240721-NB-0 #728-744 RT: 5.21-5.32 AV: 17 SB: 19 0.03-0.16 NL: 2.15E7
T: + c ESI Q1MS [50.000-500.000]
60.06
81.57
90.49
125.01
130.11
147.00
158.06
172.11
183.05
207.05
228.96
263.06
296.03
301.02
321.14
330.87
359.10
384.00
397.17
419.12
441.20
463.19
482.32
m/z
HO
O
P16

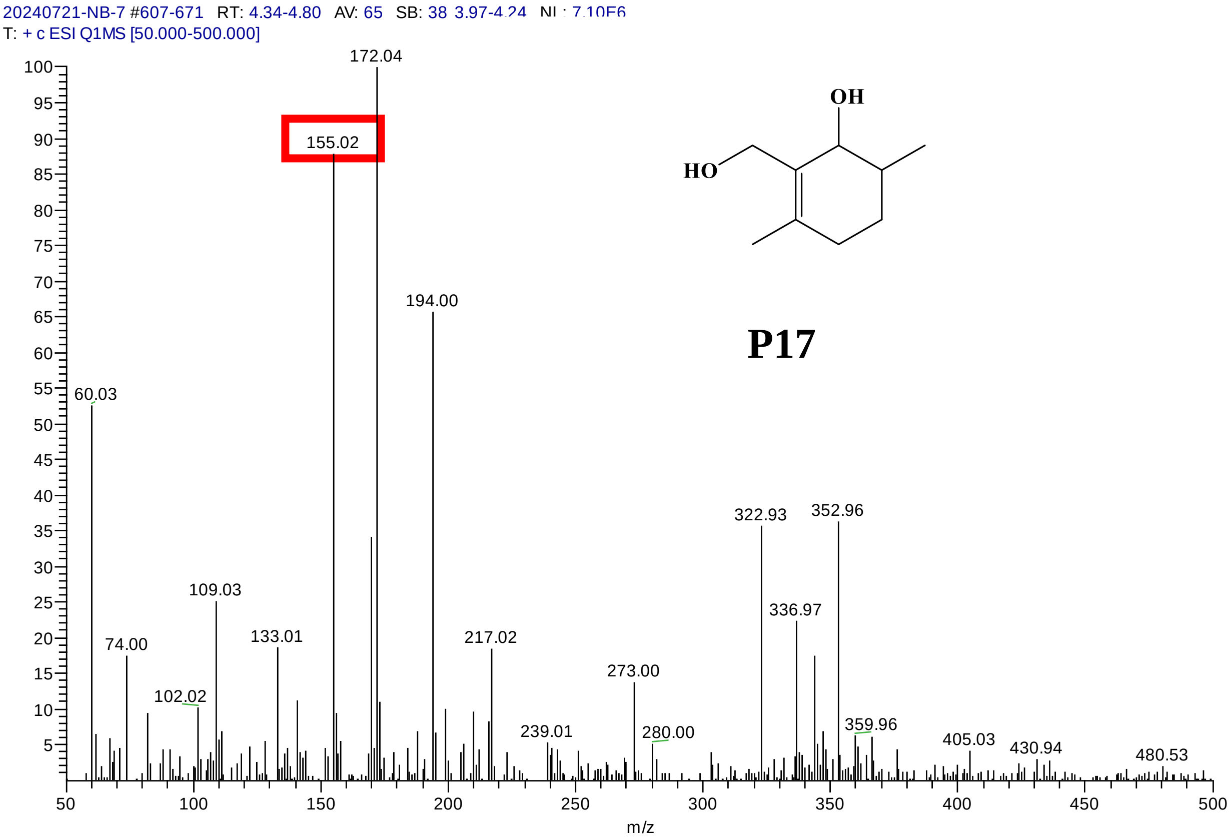
20240721-NB-7 #607-671 RT: 4.34-4.80 AV: 65 SB: 38 3.97-4.24 NL: 7.10E6
T: + c ESI Q1MS [50.000-500.000]
60.03
74.00
102.02
109.03
133.01
155.02
172.04
194.00
217.02
239.01
273.00
280.00
322.93
336.97
352.96
359.96
405.03
430.94
480.53
m/z
HO
OH
P17

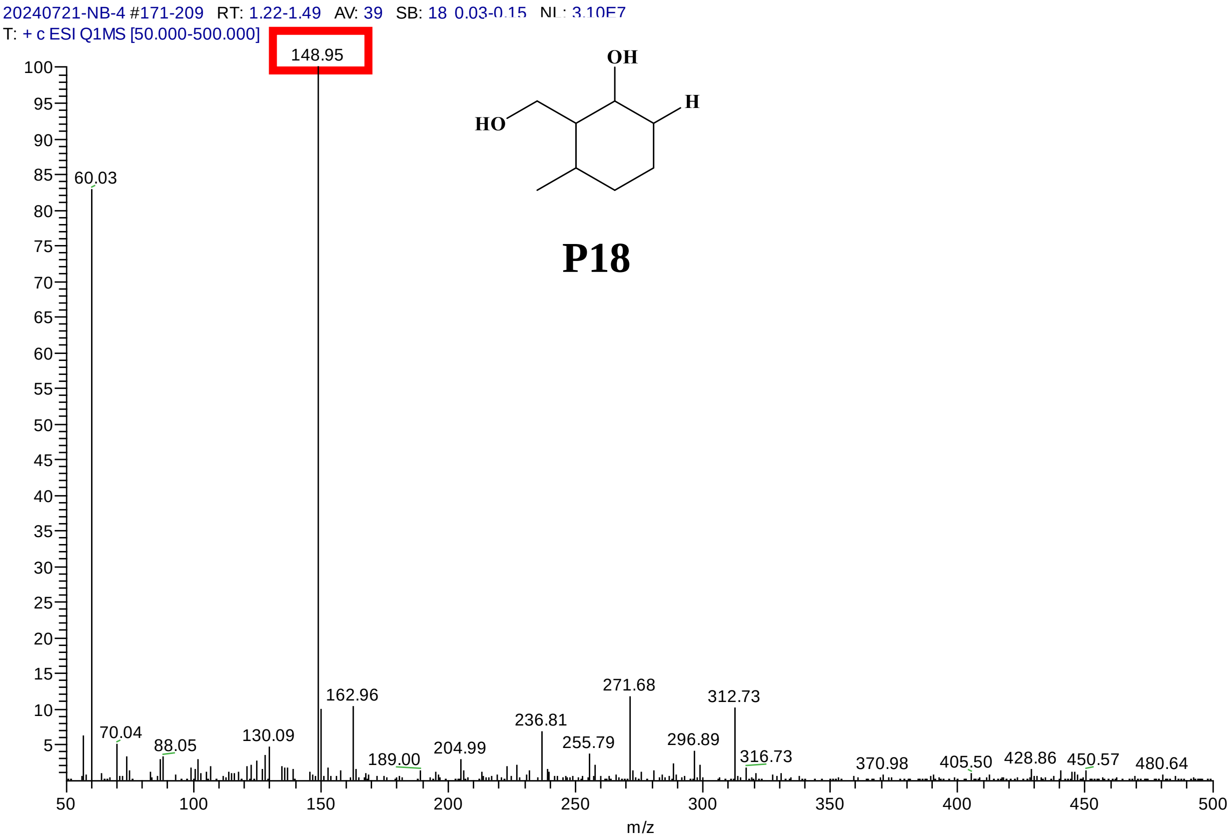
20240721-NB-4 #171-209 RT: 1.22-1.49 AV: 39 SB: 18 0.03-0.15 NL: 3.10E7
T: + c ESI Q1MS [50.000-500.000]
148.95
60.03
70.04
88.05
130.09
162.96
189.00
204.99
236.81
255.79
271.68
296.89
312.73
316.73
370.98
405.50
428.86
450.57
480.64
m/z
OH
H
HO

P18

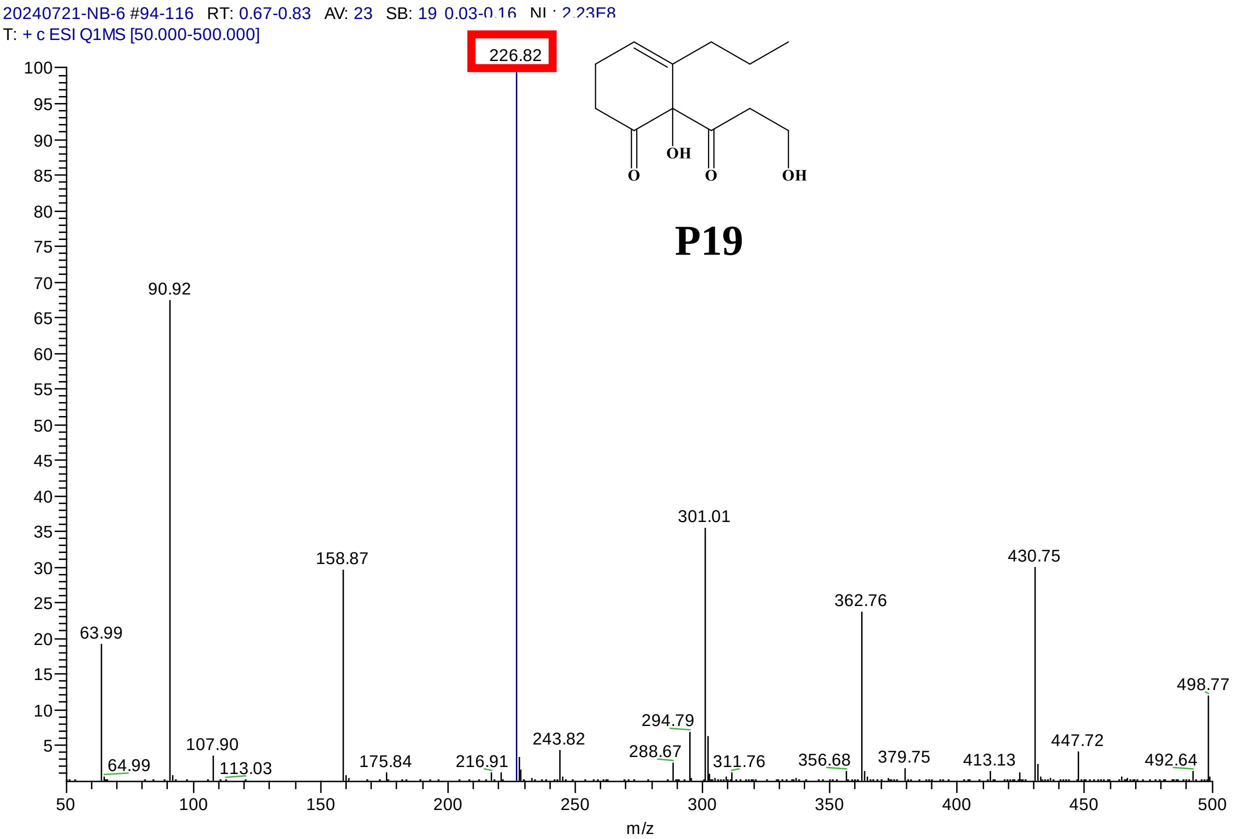
20240721-NB-6 #94-116 RT: 0.67-0.83 AV: 23 SB: 19 0.03-0.16 NL: 2.23E8
T: + c ESI Q1MS [50.000-500.000]
226.82
90.92
63.99
64.99
107.90
113.03
158.87
175.84
216.91
243.82
288.67
294.79
301.01
311.76
356.68
362.76
379.75
413.13
430.75
447.72
492.64
498.77
m/z
OH
O
O
OH

P19

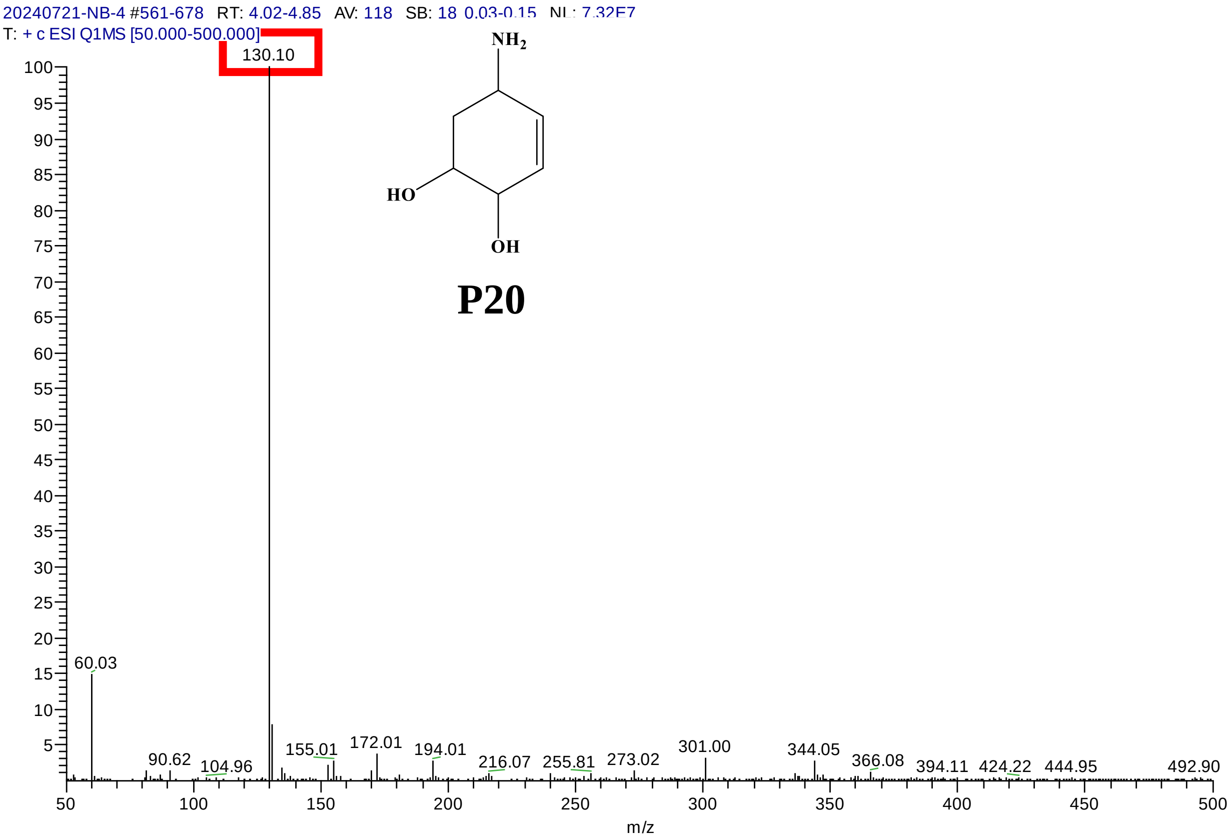

20240721-NB-4 #561-678 RT: 4.02-4.85 AV: 118 SB: 18 0.03-0.15 NL: 7.32E7
T: + c ESI Q1MS [50.000-500.000]
130.10
NH2
HO
OH
P20
60.03
90.62
104.96
155.01
172.01
194.01
216.07
255.81
273.02
301.00
344.05
366.08
394.11
424.22
444.95
492.90
m/z

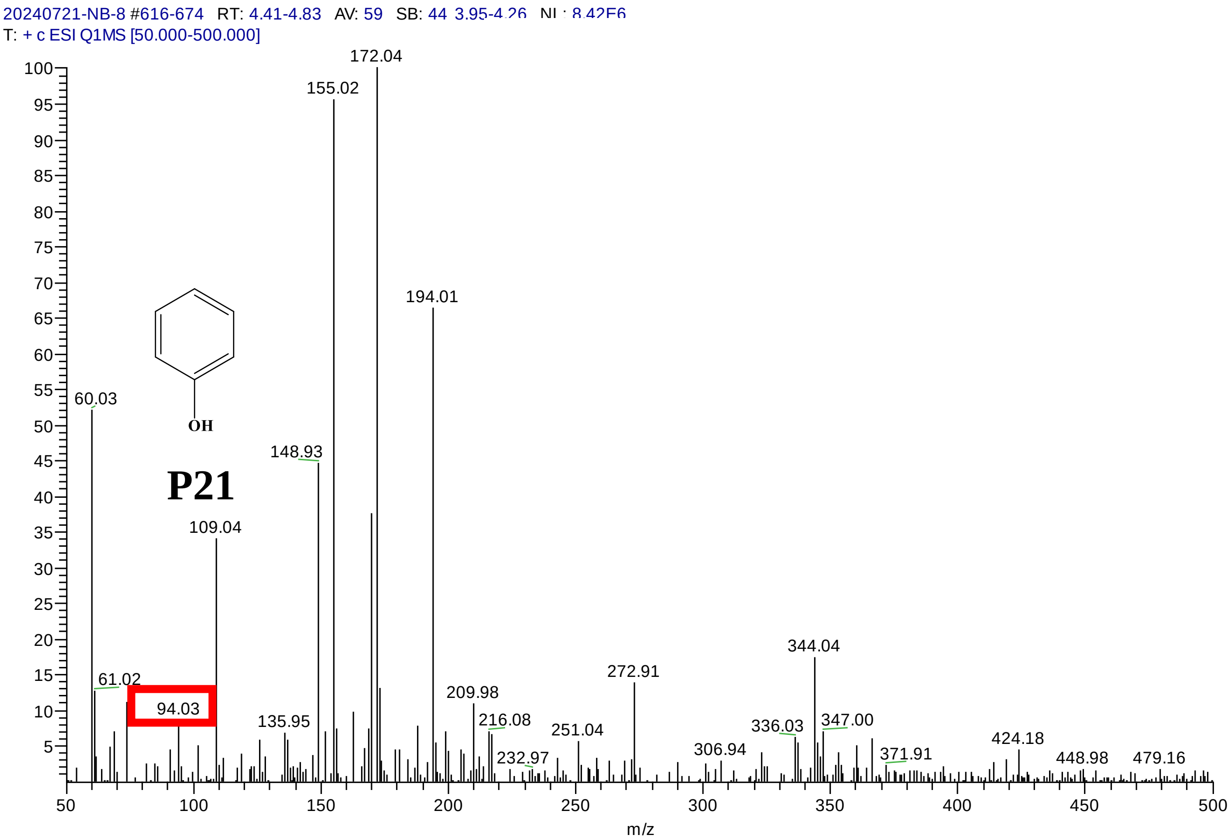

20240721-NB-8 #616-674 RT: 4.41-4.83 AV: 59 SB: 44 3.95-4.26 NL: 8.42E6
T: + c ESI Q1MS [50.000-500.000]
172.04
155.02
194.01
60.03
OH
P21
148.93
109.04
61.02
94.03
135.95
209.98
216.08
232.97
251.04
272.91
306.94
336.03
344.04
347.00
371.91
424.18
448.98
479.16
m/z

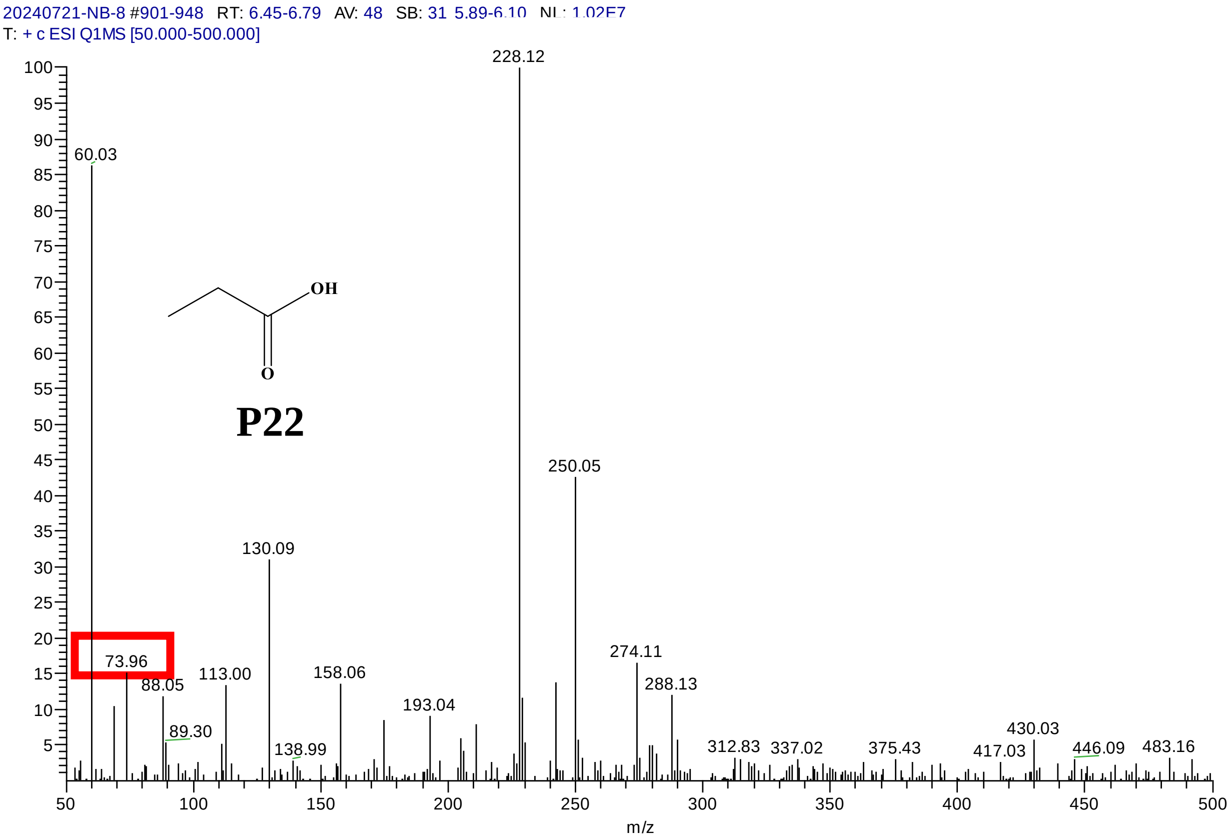
20240721-NB-8 #901-948 RT: 6.45-6.79 AV: 48 SB: 31 5.89-6.10 NL: 1.02E7
T: + c ESI Q1MS [50.000-500.000]
OH
O
P22
228.12
60.03
250.05
130.09
274.11
73.96
88.05
113.00
158.06
288.13
193.04
89.30
138.99
430.03
312.83
337.02
375.43
417.03
446.09
483.16
m/z

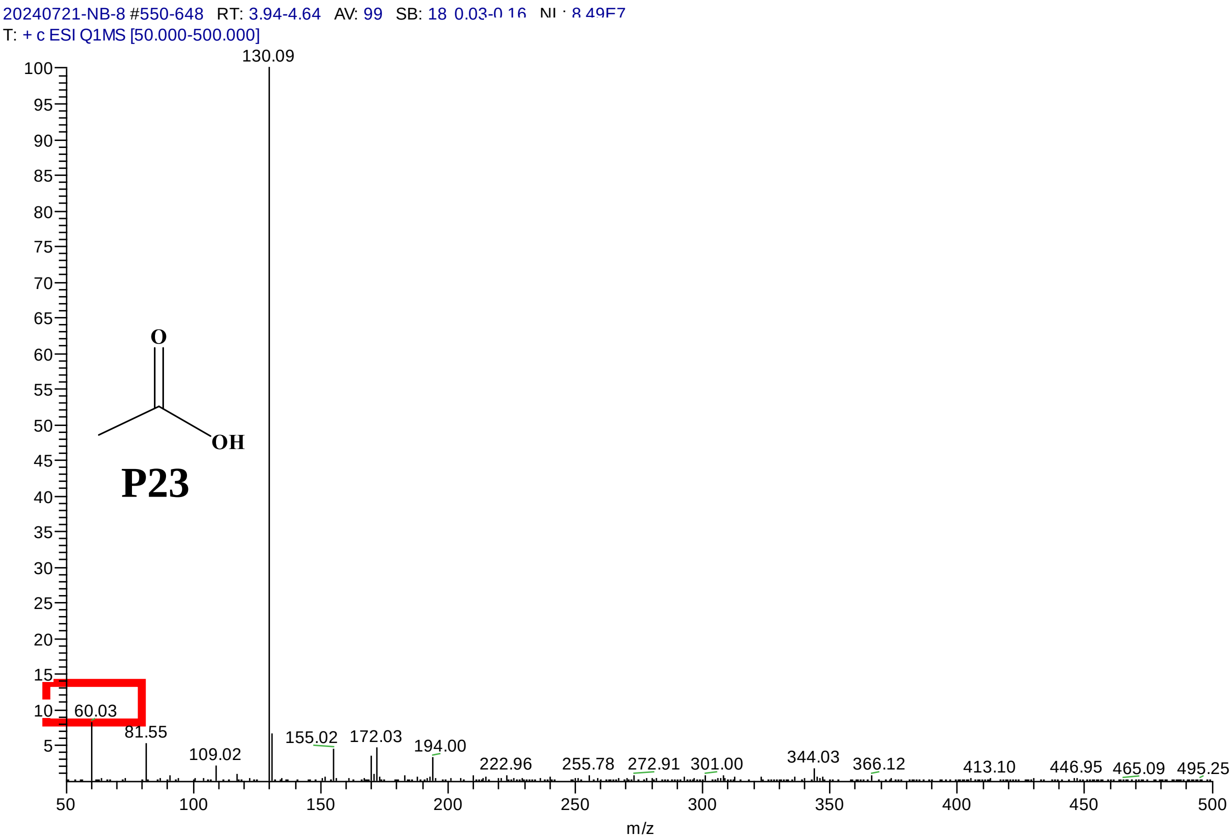
20240721-NB-8 #550-648 RT: 3.94-4.64 AV: 99 SB: 18 0.03-0.16 NL: 8.49E7
T: + c ESI Q1MS [50.000-500.000]
130.09
O
OH
P23
60.03
81.55
109.02
155.02
172.03
194.00
222.96
255.78
272.91
301.00
344.03
366.12
413.10
446.95
465.09
495.25
m/z